HORIZON 2020

THEME SC5-2017

EUCP
European Climate Prediction system

(Grant Agreement 776613)

European Climate Prediction system (EUCP)

Deliverable D3.5

Outer-European domain simulations

Deliverable Title	*Outer-European domain simulations*	
Brief Description	*We report on a set of convection-permitting climate simulations conducted as part of EUCP for three outer-European domains: (1) The Caribbean, (2) la Réunion and (3) Canary Islands and Madeira. These simulations were not foreseen in the original "Description of Action". In addition to a basic description, some basic analysis is included.*	
WP number	3	
Lead Beneficiary	*Hylke de Vries (KNMI)*	
Contributors	*Erwan Brisson (CNRM)* *Marie-Estelle Demory (ETHZ)* *Marianna Adinolfi (CMCC)* *Erik van Meijgaard (KNMI), Danijel Belusic (SMHI), Fredrik Boberg (DMI), Thomas Frisius (Gerics), Abraham Torres (ICTP)*	
Creation Date Version Number Version Date	*24/11/2021* *1.0* *19/04/2022*	
Deliverable Due Date Actual Delivery Date	*31/05/2022* *26/04/2022*	
Nature of the Deliverable	R	*R – Report*
		P - Prototype
		D - Demonstrator
		O - Other
Dissemination Level/ Audience	X	*PU - Public*
		PP - Restricted to other programme participants, including the Commission services
		RE - Restricted to a group specified by the consortium, including the Commission services
		CO - Confidential, only for members of the consortium, including the Commission services

Version	**Date**	**Modified by**	**Comments**
0.0	24/11/2021	Hylke de Vries	Initial document
0.1	21/03/2022	Hylke de Vries	Merged three main sections
0.2	02/04/2022	Hylke de Vries	Addressed all comments by co-authors
1.0	19/04/2022	Hylke de Vries	Submit to EUCP Coordinator

Table of contents

1. Executive summary

The ensemble of European convection-permitting (CP) regional climate simulations forms the heart of WP3 of EUCP. These simulations were conducted for various European domains covering most parts of the European continent. During the second year of the project the EU requested the contributing partners to examine the possibility to create another set of CP-simulations for a number of additional "outer-European" domains. For many groups this was a major undertaking with minimal budget and involved setting up their modelling environments to new and often challenging environments. The present report provides an overview of this endeavour, and describes and summarises the *additional* "outer-European" CP regional climate simulations.

The three domains that were selected are: 1) The Caribbean 2) The island of La Reunion 3) The Canary Islands and Madeira. Each of these domains comes with specific environmental challenges that require simulations at convection-permitting scales to identify and quantify the future changes that await them. As these simulations were not foreseen in the original EUCP "Description of Action", they are designed as 'demonstrators' of the application to CP-modelling to these outer-European domains, which are necessarily limited in scope and design. A short summary per domain is given below.

When designing the **Caribbean** simulations, the focus was on *Tropical Cyclones* (TCs), the main hazard in the area. TCs are accompanied with extremely strong winds, storm surges (analysed in WP4) and very intense precipitation often leading to landslides and flooding. They have fine-scale structure that would potentially benefit from a CP-modelling approach. A total of 5 groups provided simulations using 6 different model configurations (4 CPMs and 2 RCMs). Because of the large interannual TC-variability, it was decided to adopt a pseudo-global warming (PGW) approach (Schär et al. 1996). In the PGW experiments the boundary information for the regional climate model is taken from ERA5, selecting years with historically high TC-activity such as 2017. Each group simulated at least 10 of these preselected seasons. In addition to a reference simulation, a second simulation is performed in which a seasonally varying delta-change signal is added, while retaining the same daily variability as in the reference run. To our knowledge we created the *first multi-model convection permitting regional climate ensemble for the Caribbean*. Preliminary analysis has been carried out for wind speed extremes, TC damaging-potential and precipitation (climatology and hourly extremes). An important outcome is that whilst TCs are in some way 'futurized' under the PGW approach, a one-by-one comparison of a TC and its 'futurized' representation is generally not recommended. For example, randomly induced track differences may determine the sign of the along-track future changes. This emphasises the need for using an ensemble-approach. The data has been shared with WP4 for further impact analysis (storm surges). Furthermore, an EUCP storyboard has been created[1] and a paper is in preparation (De Vries et al., 2022).

Extreme precipitation and tropical cyclones also play a key role for the island of **la Réunion**, the second outer-European domain that was studied. La Reunion is a small but densely-populated island involving very steep topography (up to 3000m). This results in extremely large contrasts in precipitation, ranging from 450 mm/year on the western side up to 11,000 mm/year on the eastern side. Resolving such huge contrasts and investigating the possible future changes thereof requires modelling at fine spatial scale. CNRM conducted two 20-year (present-day and future) regional climate simulations at CP and

[1] See https://eucp-project.github.io/storyboards/carribean

non-CP resolution, to explore the effect of a better representation of orography and processes like atmospheric convection on the climate. Results indicate a robust west to east drying-to-wetting gradient over the island and a future temperature increase that is stronger in the CP-simulations than in the non-CP simulations. Furthermore, the CP-simulations resolve tropical cyclones hitting the island in much greater detail than the non CP-simulations.

Also, for the third outer-European domain (**Canary islands and Madeira**), wind and precipitation were among the key variables of interest. This region is uniquely challenging because of the combination of the small size of the islands and the high topography. Moreover, in between the islands so-called wind vortex-streets develop frequently. One of the questions was to what extent these would be resolved by climate models at convection-permitting resolution. Two groups (ETH and CMCC) contributed with simulations over this domain. ETHZ conducted a PGW-simulation at 1.1km resolution, while the simulations by CMCC were conducted using the conventional time-slice approach using EC-Earth as driving GCM. The time-slice approach simulations (CMCC) show a decrease in the annual precipitation over the region. Although an increase in autumn precipitation extremes (99.9%) is seen over Madeira, the region is known to be influenced by large-scale interannual variability (like NAO) and longer simulations are needed to examine the robustness of this result. ETH analysed the occurrence of wind vortex-streets near Madeira using very-high resolution simulations of the current climate. Key findings here are first of all that their CP-model is able to generate the vortex-streets. However, again there is large interannual variability associated with variability in the large-scale forcing. A paper summarising the key results is in preparation (Gao et al. 2022).

2. Project objectives

This deliverable has contributed to the following EUCP objectives (Description of Action, Section 1.1)

No.	Objective	Yes	No
1	Develop an ensemble climate prediction system based on high-resolution climate models for the European region for the near-term (~1-40 years)	X	
2	Use the climate prediction system to produce consistent, authoritative and actionable climate information	partly	
3	Demonstrate the value of this climate prediction system through high impact extreme weather events in the near past and near future	X	
4	Develop, and publish, methodologies, good practice and guidance for producing and using EUCP's authoritative climate predictions for 1-40 year timescales	X	

3. Detailed report

3.1 General introduction

This report provides an introduction to and an overview of the additional convection-permitting (CP) regional climate simulations that have been carried out as part of EUCP on three outer-European domains. These three domains are: 1) The Caribbean, 2) The island of La Reunion, 3) Canary Islands and Madeira. Since these simulations were not foreseen in the original EUCP "Description of Action", they were necessarily limited in scope and design. In addition to a basic description of the simulation strategy, some first basic analysis is also provided.

In the simulation strategy, as well as in the analysis of the simulations, the focus is on key variables and metrics where the convection permitting simulations can be expected to provide additional information. For the **Caribbean** the main attention is on the hurricane season (June-October). Because of the large interannual variability in the occurrence and strength of hurricanes, a so-called pseudo-global warming (PGW) approach was adopted (Schär et al. 1996). In such an approach the signal-to-noise is higher than in a conventional time-slice downscaling approach. We will show that, despite this approach, the tropical cyclones (TCs) might still take different tracks and therefore cannot be compared case-by-case easily. For the island of **la Réunion** the tropical cyclones also play a role, but here the additional complicating and challenging factor is to accurately resolve the details of the topography. Due to the steep topography, extremely large differences in precipitation occur between the west and the east of the island. Coarse-resolution simulations are completely incapable of capturing such features, and therefore cannot provide reliable future projections. For the **Canary islands and Madeira** intense precipitation is also a factor, which can lead to severe landslides. Coarse-resolution models are not able to represent the small islands and generally rain over the sea rather than over the islands. One therefore needs to rely on km-scale models to capture their spatial patterns properly. In between the islands, observations indicate the frequent occurrence of a phenomenon called wind vortex streets. These meso-scale atmospheric disturbances are not resolved by coarse-resolution models. One of the aims is to examine whether they can be resolved in climate models at convection-permitting resolution.

Since the simulations for the three domains were designed for different research purposes, it was found impractical to conduct a common analysis on all domains. Therefore, in the following three sections, the modelling strategy and model results are presented separately for each domain. We finish this report with some final thoughts and conclusions.

3.2 The Caribbean

[main contributor: **KNMI**. Additional input from: DMI, SMHI, GERICS, ICTP]

3.2.1 Introduction

The Caribbean is a large region in the western part of the tropical and subtropical Atlantic Ocean with relatively high sea-surface temperature (SST). It contains a large number of islands that are characterised by white sandy beaches and lagoon-blue waters. The area is known for being a key region where Atlantic Tropical Cyclones form or migrate through after being formed off the west coast of Africa. Figure 3.2.1 shows a satellite image taken on September 8, 2017. The 2017 hurricane season was extraordinarily active and contained no less than 17 named storms. On this particular day, three active hurricanes could be counted in the basin, among which the landfalling major hurricane Irma.

Figure 3.2.1: Satellite image of September 8, 2017, showing three active hurricanes (from left to right Katia, Irma, Jose). Credit: NASA / NOAA (source).

While not all hurricanes meet islands or mainland, their landfall invariably has a huge socio-economic impact, including loss of life and large infrastructural damage (WMO, 2021). Coastal populations are particularly vulnerable as the devastating wind speeds associated with the hurricanes are usually accompanied by monstrous ocean waves and formidable storm surges (EUCP-WP4 deals with the storm surges). Another major impact factor is the excessive precipitation amounts associated with the hurricanes. The rain intensities and rain amounts recorded in hurricanes are very high and often induce local flooding and landslides especially on hilly terrain. Even without climate change, the societal impact of them is already increasing as a simple consequence of increasing coastal populations. Knowing the fate of tropical cyclones in a warmer climate is therefore paramount to understanding the vulnerability of coastal populations in the future.

What the future brings when it comes to tropical cyclones is not entirely clear (Emanuel, 1987, Knutson et al 2019). Two important aspects of tropical cyclones are their intensity and their frequency. Physical understanding tells us that that higher sea-surface temperature (SST) will provide more energy to tropical cyclones through increased evaporation and latent-heat release, thereby making them bigger, wetter (Clausius-Clapeyron) and more intense (see e.g., Oldenborgh et al. 2017). In the current climate, the Atlantic Hurricane season runs from June to November, but this may become longer (SST is required to be above ~26C for TCs to form). However, while SST increases under virtually all climate-change scenarios, changes in other large-scale environmental parameters may produce opposing tendencies (Vecchi & Soden, 2007). A commonly used environmental TC indicator is the Genesis Potential Index (GPI), as first described in Emanuel and Nolan (2004) and later extended in various ways (e.g., Wang and Murakami (2020) and Gilford (2021)).

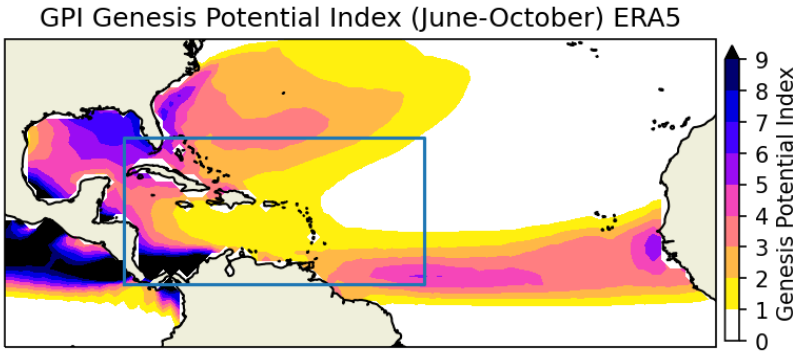

Figure 3.2.2: June-October average Genesis Potential Index (GPI) derived[2] by KNMI using ERA5 data for the period 1979-2020. The rectangle shows the approximate analysis domain of the (CP)RCM simulations.

The GPI (see Fig. 3.2.2) involves various environmental parameters such as SST, 600hPa relative humidity, the magnitude of the vertical wind shear between 200 and 850hPa, absolute vorticity at 850hPa and the so-called maximum potential intensity (MPI) which is an empirical value that integrates information from SST and the moisture and temperature profiles. GPI is used to explain spatial and temporal variability of TC-occurrence in the current climate and can therefore also provide indications of the future changes. There is growing consensus that the combined result of the competing mechanisms is that the most intense tropical cyclones (>Cat3 on the scale of Saffir-Simpson) will likely get stronger and wetter (and possibly fewer), while the less intense tropical cyclones might decrease in frequency (Knutson et al 2019). In EUCP we examine some of the future TC changes within the context of very high-resolution km-scale regional climate modelling.

3.2.2 Simulation description & methods

Table 3.2.1 lists the groups that contributed. Two simulations were performed at a horizontal resolution of around 12 km. These are referred to as the "RCM" simulations. The other simulations were conducted at a horizontal resolution of ~3-4km and are referred to as the CPM simulations. Note that the HCLIM38-ARONE simulation by DMI is run in CPM mode i.e., without deep convection parameterization, but at RCM horizontal resolution of ~12km. For this reason, it is referred to as RCM in this report. Apart from the horizontal resolution, the setup of DMI is identical to that of SMHI.

Table 3.2.1: Contributing groups and simulations (Caribbean domain).

Group	**Model**	RCM**/CPM**	**Resolution**	**Details**
DMI	HCLIM38-AROME	RCM[3]	~12km	directly in ERA5
KNMI	RACMO2.3	RCM	~12km	directly in ERA5 1979-2020, REF, TP2, PGW
KNMI	HCLIM38-AROME	**CPM**	3km	nested in RACMO-run
SMHI	HCLIM38-AROME	**CPM**	3km	directly in ERA5
GERICS	REMO-NH	**CPM**	0.04deg	directly in ERA5

[2] KNMI acknowledges Dr. Wencheng Yang for using the GPI-code (https://github.com/wy2136/TCI)
[3] See note in main text: DMI ran in CPM-mode but at lower spatial resolution.

ICTP	RegCM4-7	**CPM**	4.5km	directly in ERA5

Pseudo Global Warming (PGW) approach

It was decided to focus on the main hazard in the region, the tropical cyclones. Because TC-variability is very large, many simulation years would be necessary to properly estimate future changes in TCs. One of the influencing factors is El Niño. In years with positive El Niño, Atlantic hurricane activity is suppressed. Since these simulations were not planned at the start of EUCP, the computational resources were limited and not sufficient for such a huge undertaking. Only O(5-10) seasons could be afforded. This combination of large variability and a limited computational budget would imply that a conventional GCM-driven set of CPM/RCM simulations would most likely produce results with a low signal-to-noise ratio. At the GA in March 2020 (Trieste) it was decided to use a pseudo-global warming (PGW) approach instead (Schär et al. 1996). In the PGW approach, a reference integration is generated using reanalyses (in our case ERA5) data at lateral boundaries. A second integration is then produced by adding a seasonally varying delta-change signal to the original ERA5 lateral boundary data. The delta-change fields are taken from one or several CMIP5 GCMs and have been prepared by KNMI[4].

There are advantages and limitations to the PGW approach. One advantage is that, by using ERA5 at the boundaries rather than a GCM, one is guaranteed to apply the correct (i.e., 'observed') variability, at least insofar as they are contained in the reanalysis. Another advantage is that the (natural) variability in the large-scale drivers is unchanged in the PGW simulation. This increases the signal-to-noise ratio. Finally, with PGW one needs only two simulations (ERA5+PGW), while in a conventional approach one needs both a reanalysis-forced evaluation and two GCM-driven climate-change simulations. A disadvantage of the PGW approach, however, is that future changes in forcing variability (i.e., originating from changes occurring outside the simulation domain, for example changes in the GPI, Fig.3.2.2) are not taken into account. Therefore, the PGW approach cannot be used to conclusively address the question of the future change in for example the TC frequency. Instead, with PGW the focus is on the "futurization" of present-day weather. Still, we consider the short set of seasonal PGW simulations to be more useful than an even shorter set of simulations obtained using a conventional GCM-based approach.

Simulation setup

The analysis domain for the simulations is shown by the yellow line in supplemental figure S1. Details of the simulation domain were left to the individual groups. To reduce computational demands, it was decided to simulate 10 hurricane seasons (June-October) that were selected from 1979-2019 following a number of criteria (explained below). Summary of the simulation protocol:

- Minimal domain: 8.0N to 26.7N & -47.0E to -85.0E (Figure S1).
- Boundaries: ERA5 (3-hourly).
- Season: 1 June - 31 October (most hurricanes, though not all, occur in these months)

[4] KNMI prepared a set of common delta-change fields from a subset of 19 CMIP5 projections for the RCP8.5 scenario. The reference and future periods used for determining the delta change field were 1976-2005 and 2071-2100, respectively. More details can be found in the appendix to this section.

- Run at least 5 pre-selected hurricane seasons (details below).
- PGW-perturbation is based on 19 CMIP5 RCP8.5 models. The average increase of global air temperature is ~3.4K.

To investigate the effects of the altered circulation and spatial pattern of the warming, KNMI ran a second set of simulations with RACMO2.3 (RCM) using a spatially uniform temperature increase of 2K (keeping circulation and relative humidity constant) - referred to as TP2 in this report. In addition RACMO2.3 was run for all years between 1979 and 2020 to increase signal to noise ratio.

Gutmann et al. (2018) (referred to as G18 from here) reported on a set of CPM simulations obtained using a PGW approach. They used a larger domain that extended much further north, and ERA-Interim for lateral boundary conditions. KNMI experimented whether there was any advantage of using ERA5 above ERA-Interim by running the case of 2017 hurricane Irma with both boundary conditions. Using ERA5 was found to be more appropriate in this case. Its higher spatial (30 km versus 110 km in ERA-Interim) and time (1-hourly versus 6-hourly) resolutions led to an improvement of the simulation of the hurricane Irma that entered the domain at mature stage[5].

Selection criteria

The final step was to select a set of ERA5 years to be downscaled. At the EUCP General Assembly in March 2020, it was decided to base this selection on the IBTrACS hurricane observation database. KNMI created a top-10 list of candidate seasons following three criteria (Figure 3.2.3). Among the selection is the recent extraordinary year of 2017, but also other well-known years featuring devastating hurricanes. Note that one of the requirements of the selection procedure was that the track of the hurricanes went to nearby land areas (island or mainland). The reason for applying this criterion was that in this way the results would also be relevant to WP4 and the impact community. The top-10 has 19 TCs above Cat2 (within blue box and nearby land).

[5] An animation of the MSLP field of hurricane Irma simulated with RACMO RCM, using ERA5 or ERA-Interim as lateral boundary conditions, can be found here.

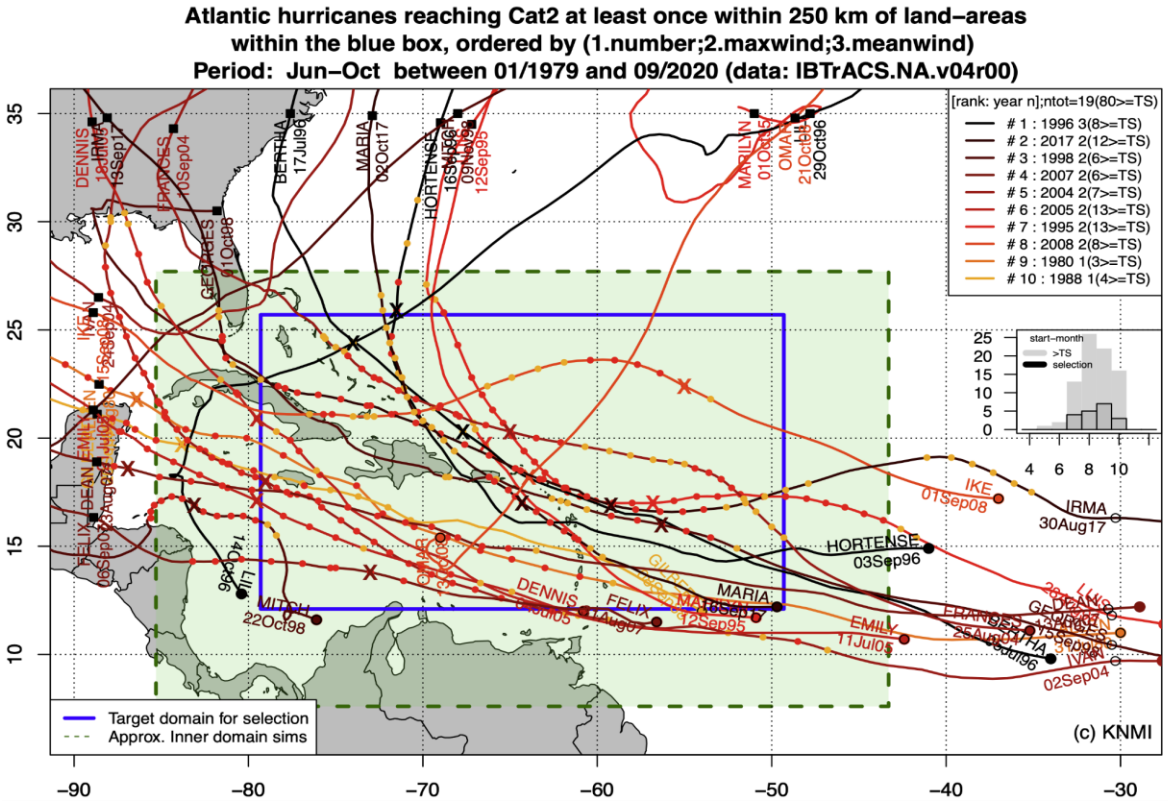

Figure 3.2.3: Hurricane tracks extracted from the IBTrACS database. The title in the figure shows the criteria that were used to create the top-10 list of selected seasons shown in the top-right. Dots indicate star tdate of events in the database (open dots enter plot domain already existing), and boxes the end of trajectories. Big crosses denote approximate location of storm maximum wind speeds (coloured circles in orange and red indicate the time-instances where TC-intensity is above Cat3 and Cat4 respectively). The inset shows the number of cases (TS indicates Tropical Storm criterion).

PGW delta-change fields

Figure 3.2.4 shows some of the CMIP5-based delta-change fields (June-October average) and the equivalent ERA5-based variables in the control climate (contours). The latter are taken from the 10 years that contributed to the analysis. Surface temperatures increase on average between 2 and 4 degrees (top-left). At height the increase is stronger leading to increased vertical stability (top-right). Mid-tropospheric relative humidity decreases (bottom-left). Finally, the vertical shear of the zonal wind shows a mixed pattern (bottom-right). Increased shear is another limiting factor for TC-development. Note that in the additional set of 'uniform-warming' TP2-simulations by KNMI, relative humidity is kept constant and the systematic circulation changes are absent.

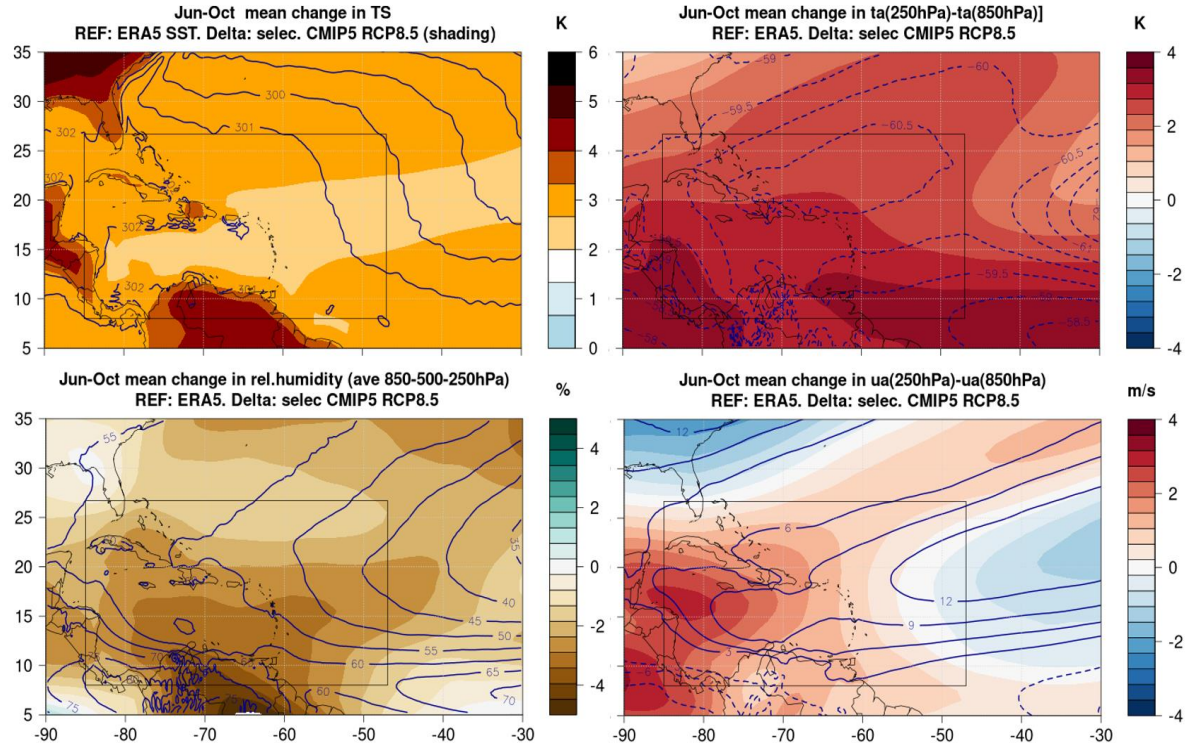

Figure 3.2.4: June-October ensemble-mean PGW-delta change fields (shading) derived from a selection of CMIP5 RCP8.5 models. Contours show control values (using June-October averages of the simulation years) taken from ERA5. Top-left: surface temperature (contours: SST), top-right: change in temperature stratification (250hPa-850hPa). Bottom-left: change in relative humidity (vertical average of data at 850-500-250hPa), bottom-right: change in the vertical shear of the zonal wind (250hPa-850hPa).

3.2.3 Results

In this section we present the first results. We start with an evaluation of hurricane Irma (2017) in the models. This is followed by a common analysis of wind speed and precipitation.

3.2.3.1 Evaluation (Hurricane Irma)

In September 2017 the Caribbean was hit by major hurricane Irma. Irma formed east of our simulation domain and propagated into the region as a mature storm, with recorded wind speeds already well over 50 m/s. We use this case to evaluate our ensemble since we expect all models to resolve the case. Short test simulations (starting on 1 September rather than 1 June) by KNMI showed a good match to the observations of the track (see Irma's hourly wind field test simulation for an animation). However, in the climate runs (starting in June of each year), the spin up period is longer and because the TCs are allowed to roam quasi freely in the interior of the domain, it is not guaranteed that after entering the domain the tracks stay close to the observations.

Figure 3.2.5 shows the evolution of Irma in terms of the track (top panel), minimum MSLP (bottom right panel) and maximum W10MAX (maximum hourly 10m wind speed, bottom-left panel). In this figure, the observations were taken from the IBTraCS database.

All models simulate hurricane Irma after it entered the domain. Initially the tracks are close together, but their spread increases with time, somewhat resembling an ensemble weather forecast. Especially

in RegCM4-7 Irma remains 'spot on' in terms of the track. For the other major hurricane of 2017 ('Maria') the ensemble spread was noticeably larger.

The evolution of MSLP also differs (bottom-right panel Fig. 3.2.5). While both RACMO2.3 and KNMI/HCLIM38 follow the observed MSLP minimum quite well initially, their pressure drop at later stages is too strong. This is likely a consequence of the northerly trajectory in the simulation with these two models that keeps Irma sea-bound. In the observations Irma is closer to the islands, which limits intensification. The other models are generally offset significantly in MSLP. This offset is probably caused by the boundary forcing (ERA5), which itself does not resolve Irma very well: The ERA5 MSLP-minimum is ~10-20 hPa higher at the time of entrance in the domain. RACMO2.3 suffers less because its simulation domain extends further eastward. As a consequence, Irma had more time to spin up, before entering the analysis domain. KNMI/HCLIM38 benefits from this because it is run nested within RACMO2.3. All other models run directly using ERA5. Although an MSLP-minimum can be tracked in ERA-Interim, there is hardly any development. This is another confirmation that it is better to use ERA5 than ERA-Interim. The large model-spread in MSLP illustrates that objective TC-tracking using a fixed MSLP-threshold might not be an option.

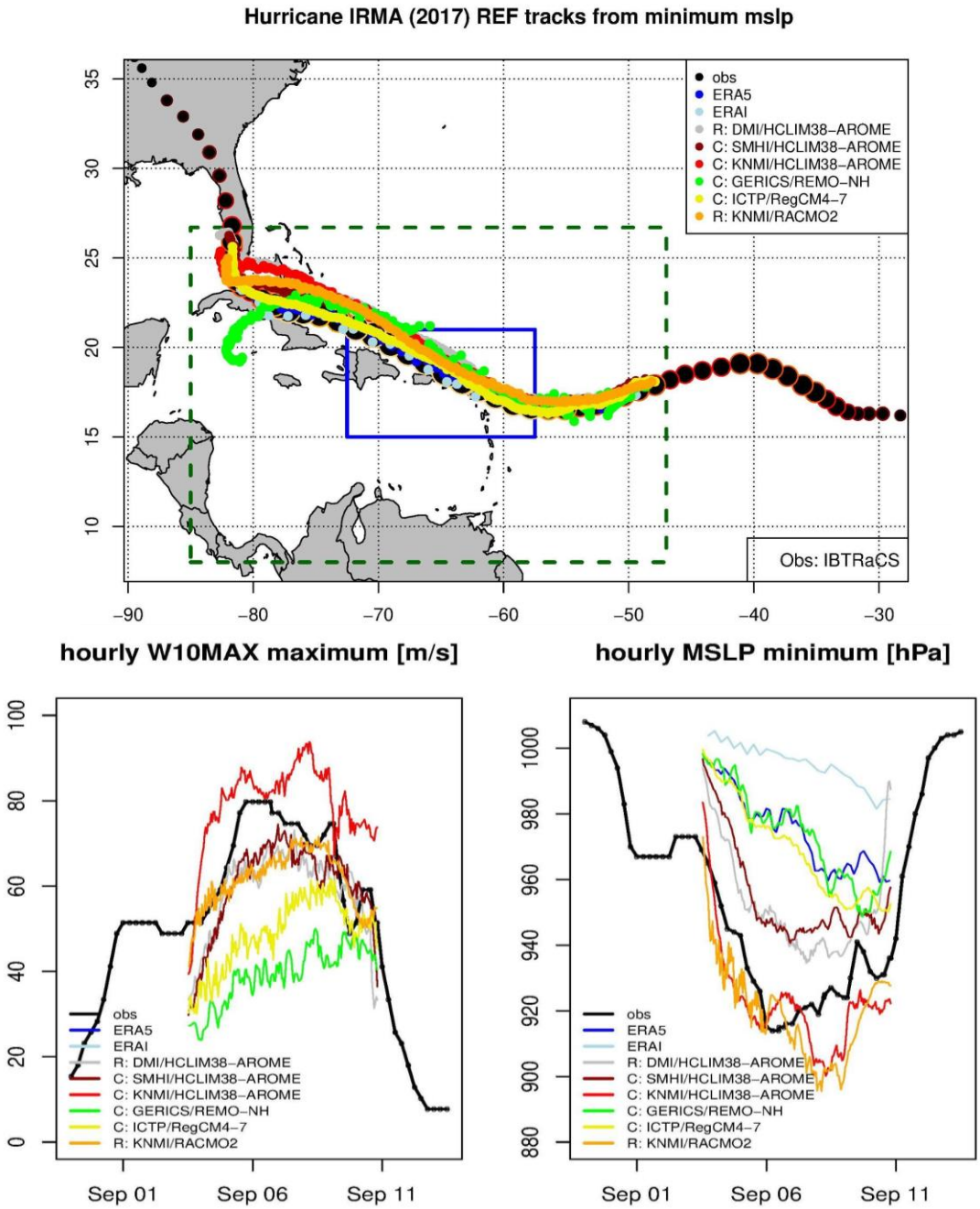

Figure 3.2.5: Hurricane Irma (2017). The top-panel shows the tracks as diagnosed by the minimum in MSLP. Bottom-panels show evolution of (left) W10Max (maximum hourly wind speed, excluding gusts; for ICTP Hourly snapshots are used, ERA5 and ERA-I not shown); (right) Minimum MSLP.

Wind speed maxima (W10MAX) are shown in the bottom-left panel Fig. 3.2.5 (note that ERA5 and ERA-Interim are not displayed). KNMI/HCLIM38 stands out with too high maxima, but again its too northerly track is partly causing this. Both 12-km simulations (KNMI/RACMO2 and DMI/HCLIM38) score quite well and so does the high-resolution HCLIM38 version run by SMHI. If we recall that the only difference between DMI/HCLIM38 and SMHI/HCLIM38 is the difference in the horizontal resolution (12-km versus 3-km), their similarity (in these parameters) shows that a 12-km resolution convection-permitting setup may be quite suitable for simulating TCs realistically. In the ICTP simulation with RegCM-4.7 the minima are found to be lower, but this may be partly a consequence of the output being an hourly snapshot rather than the hourly maximum. Finally, REMO-NH produces

the lowest W10MAX. In that model the structure of Irma seems also less well resolved (and of larger spatial scale). Viewed together, however, the mini ensemble can be said to capture the observations reasonably well.

Hurricane Irma under PGW

In the PGW-simulations the trajectories diverge more (Fig. 3.2.7). Especially in RACMO2.3 and KNMI/HCLIM38 Irma reaches further north. The other track changes are smaller, except for REMO-NH in which Irma eventually curves south, seemingly unable to exit the domain. This "stalling" behaviour is seen more often near the edge of the domain and not only in REMO-NH, and is probably related to the modified boundary conditions.

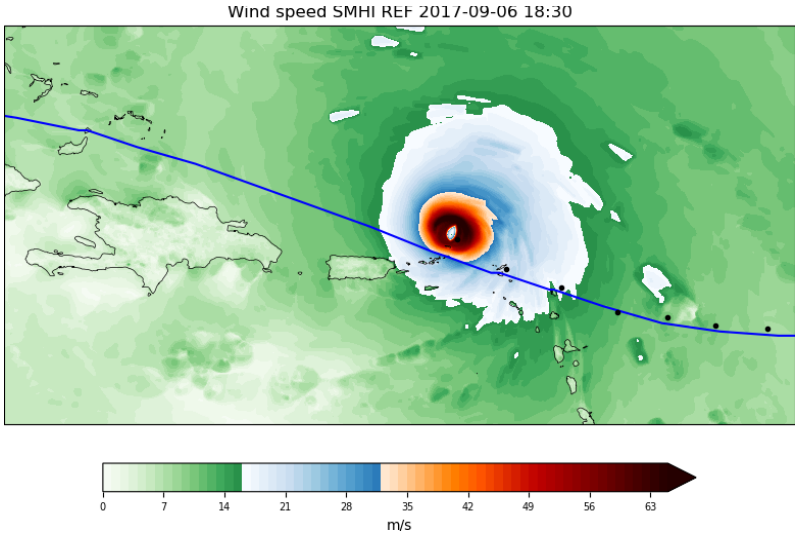

Figure 3.2.6: Snapshot of W10MAX field in the reference simulation of SMHI. The track from IBtrACS is indicated by the line.

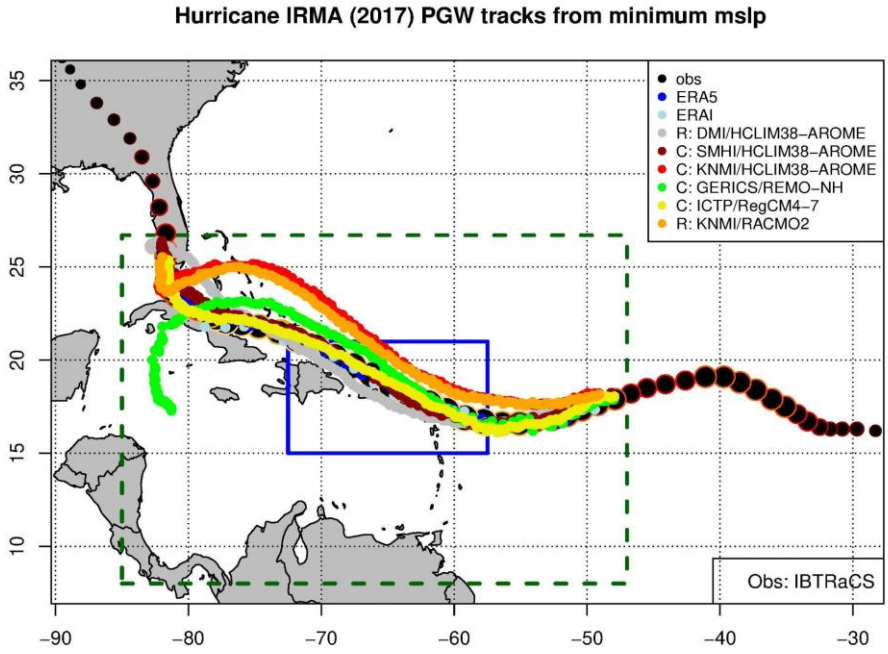

Figure 3.2.7: Trajectories of hurricane Irma in the PGW simulations.

The MSLP and W10MAX intensity of Irma do not change much under PGW (Fig. S2), except in those simulations in which Irma is more sea-bound under PGW (i.e., for the KNMI and GERICS runs, the MSLP minimum is deeper and W10MAX increases). Apparently, the SST increase that would potentially fuel Irma, is compensated by inhibiting factors from changed tropospheric relative humidity, stabilisation and wind-shear.

There is, however, another more fundamental reason why a TC like 'Irma' that is 'futurized' using a PGW-approach, does not necessarily become stronger. From a statistical point of view Irma was an extreme that formed under current-climate conditions that were 'just right': the right SST, the right shear, humidity, etc. If at a certain point in its life-cycle the large-scale environmental factors of such an extreme are changed – albeit even weakly – this could well bring it "out of balance" and thereby make it less extreme. This intrinsic property of the PGW-approach may prove problematic, in particular in event-based applications, and must therefore be a recurring point of attention when using the technique to for example the future changes of observed precipitation extremes (See also EUCP work by D. Matte on the Copenhagen precipitation extremes). Therefore, it is generally not recommended to derive the future-change signal from single cases.

3.2.3.2 Wind speed extremes and hurricanes

10m wind speed maxima (W10MAX)

One way to make the results more robust is to aggregate over time and/or over space. For each grid-point and season we computed the number of hours in which the Cat1 threshold (32.6 m/s) is exceeded in W10MAX. This particular statistic is shown here for RACMO2.3/KNMI for which we have more years (1979-2019) and three data sets (REF, PGW and TP2) available. The left panel in figure 3.2.8 shows the spatially aggregated results. In the PGW run (black dots) the frequency is on average lower than in REF. On the other hand, a very robust increase occurs under TP2, i.e., if the influence of

a changing large-scale circulation and relative humidity is excluded. This decrease under PGW is seen also for the other models (not shown). The maps at the right show the spatial structure (maps for the other models are available upon request). The Northwestern part of the domain is most favoured for the occurrence of high wind speed.

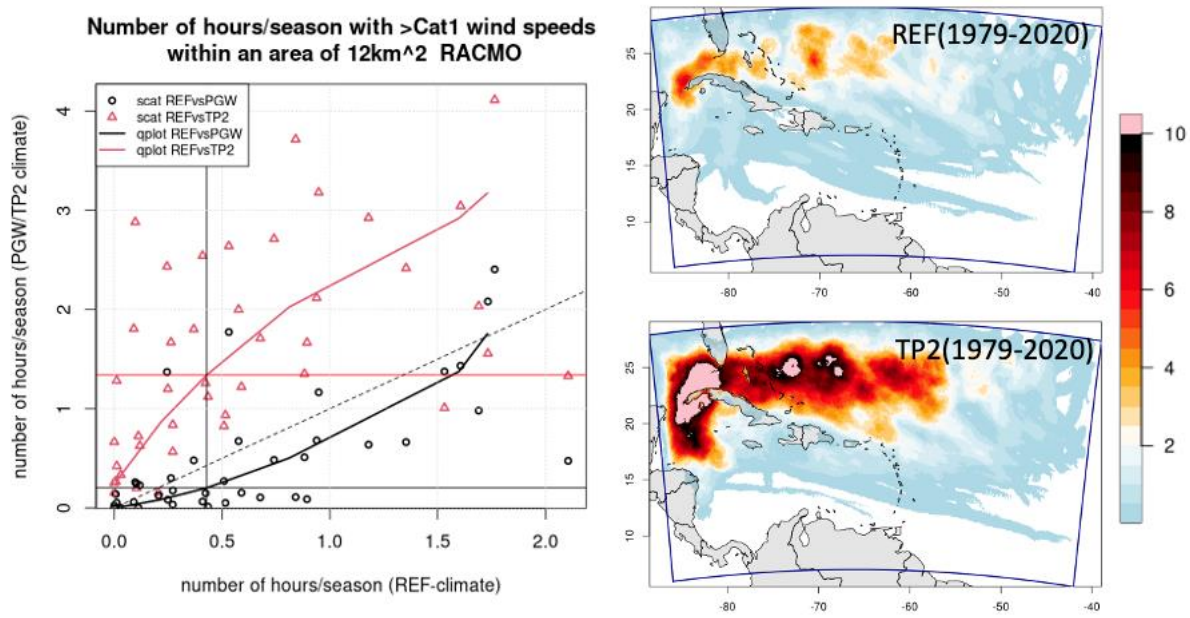

Figure 3.2.8: Number of hourly maximum wind speeds (W10MAX) above Cat.1 in RACMO. Left: scatter plot (each dot represents one simulation season June-October). The lines connect the quantiles, horiz/vert. lines indicate P50. Right: spatial maps of gridpoint-based mean seasonal number of hours above Cat.1.

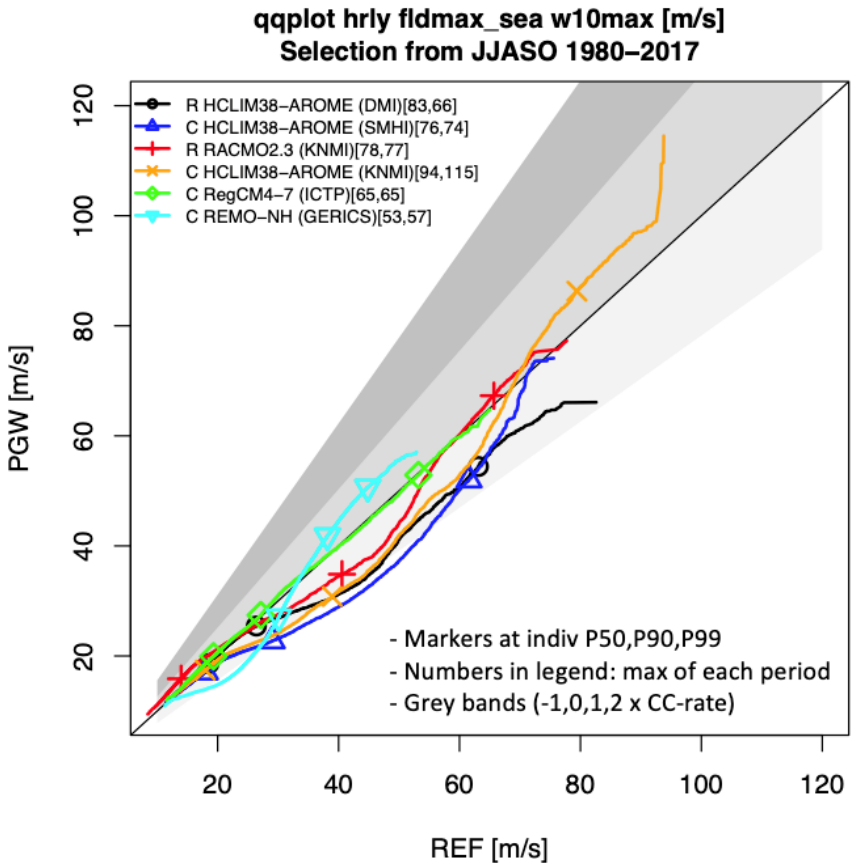

Figure 3.2.9: Quantile-quantile plot of the spatial maximum of hourly W10MAX (sea areas only). The grey bands indicate scaling behaviour with n=(-1, 0, 1, 2) x Clausius-Clapeyron (7% per degree warming).

Finally, we consider the distribution of the hourly highest W10MAX occurring anywhere in the domain (sea only). Here all models are included. Figure 3.2.9 shows a quantile-quantile plot (qqplot) for the REF and PGW distributions. If the qqplot falls below the *y=x* line it implies that PGW produces systematically lower hourly field maxima. This occurs for the majority of the models in the 20-60m/s range (exceptions are REMO-NH, which shows increases in this range, and RegCM4-7 which is almost 'flat' implying no distribution change at all). In the far-right tail of the distribution, most models hint on a neutral or even positive change, but this signal seems too noisy to put high confidence in.

Tracking hurricanes

A tracking analysis of the entire CPM/RCM ensemble was not possible in the time available. KNMI conducted a TC-tracking of their RCM simulations with RACMO2.3 for which more years and two scenarios are available (PGW and TP2). The tracking software used is *celltrack* (Lochbihler et al. 2017). Following G18, tracks are initiated if MSLP falls at least 17hPa below the local yearly maximum MSLP and W10MAX>15m/s in a region around the MSLP minimum. A track is kept if min(MSLP) falls 27hPa below the year-maximum at least once, the track-duration is at least 3 hours and max(W10MAX) exceeds 25 m/s.

G18 analysed 22 TCs within the PGW-framework using a single CPM (WRF model). These were not the only TCs that developed during their simulations, only those that were having a track close enough to the historic record in both simulations. It is an open question whether the other TCs that form, either spontaneously within the domain, or that deviate strongly from the historic record, should be

discarded. In the other statistics shown in this chapter, such as for example the precipitation climatology and the wind extremes, they are of course included implicitly. For this reason we retained *all* TC that occurred within the domain.

One of the outcomes of G18 is that there is considerable spread within their ensemble of TC responses: some TC strengthen under PGW, while others weaken. Only for a few cases they could diagnose statistically significant differences, but the most robust results were found when all storms were pooled together. In the previous section we already saw that this also occurs in our CPM-RCM ensemble.

Basic findings (for RACMO2.3/KNMI only) are:

- Compared to REF, the absolute number of tracked hours is reduced in PGW but increased in TP2. Especially in TP2 new TC form occasionally in the domain. The tracks of the major TC are usually comparable, but similar to G18 it is generally not possible to derive statistics by looking at individual cases.
- Precipitation intensities: robust frequency increases of the highest precipitation intensities, *both* in TP2 and PGW. This is probably the most robust metric.
- MSLP-minima and W10MAX-maxima: distributions broaden. Both intensifying and weakening storms are found (mostly weakening under PGW). This is partly due to subtle shifts in the tracks.
- TC-radius and translation speed: only in TP2 the frequency of TC with a large radius increases. Furthermore, there are *no* clear signs of weakened translation speeds in the region of our simulations, as reported for example in Kossin (2018) and G18. G18 found a reduction of translation speed in their PGW experiments, but this is not confirmed by the RACMO2.3 simulations.
- Cyclone Damaging Potential (CDP): This metric combines translation speed, intensity and radius into a damaging potential (Holland et al. 2016). Absolute frequency decreases are found in all CDP-classes for the PGW experiments (not shown). In contrast, increases are seen in TP2 in all CDP-classes. Relative frequency increases in the strongest GDP-classes are only seen in TP2 (Fig. 3.2.10).

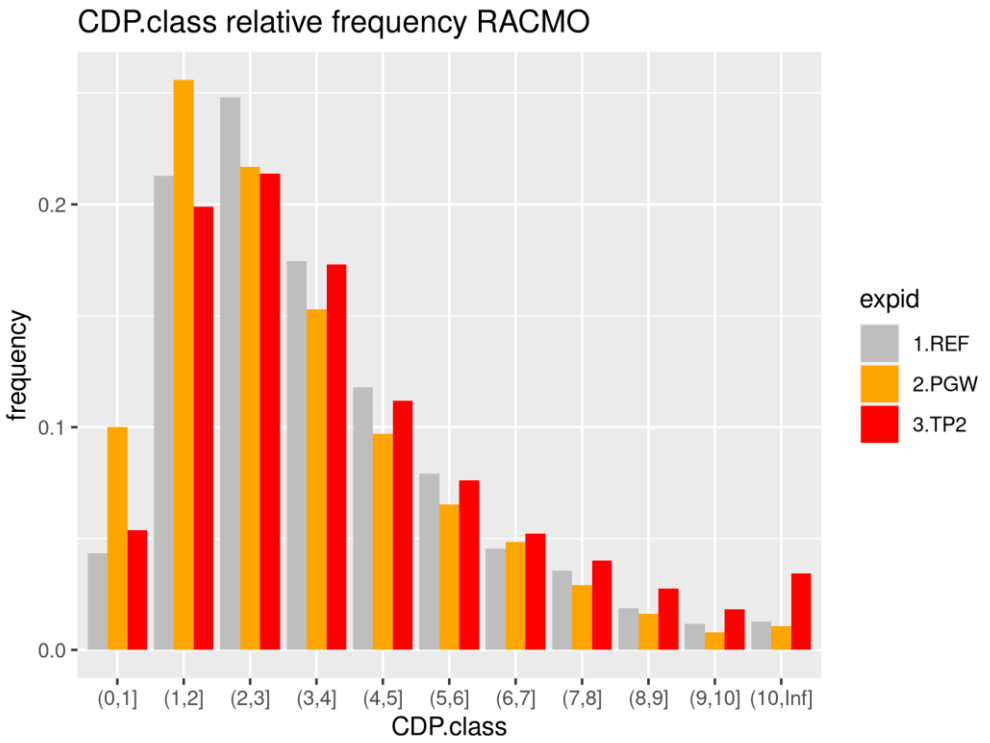

Fig. 3.2.10: Cyclone damaging potential (CDP, higher means "more damaging") histogram, obtained from the tracking analysis of the RACMO2.3 simulations. All years (1979-2019) are used. Results are shown as relative fraction per simulation.

The tracking results were compared to the data from the IBTrACS database (such as radius, intensity and translation speed). However, because the criteria could not be matched exactly, a completely quantitative comparison was found to be quite difficult. A more complete overview of the tracking results will be described in De Vries et al. (*in preparation*).

3.2.3.3 Precipitation - climatology and hourly extremes

Climatology

First, we have a look at the precipitation climatology. Precipitation is averaged over all months (June-October) and available years. Model output is compared to monthly satellite data from GPCP (Adler et al. 2016) and to ERA5, using the same years as those used in the simulations. Two further observation data sets are explored, the rain gauge-based CPC set[6] (land only) and the high-resolution merged satellite product GPM IMERGE[7]. The latter is only available after 2000, but has the advantage that it is of daily time resolution such that metrics like wet-day frequency can also be computed. The three observation sets and ERA5 are shown in the top four panels of Fig. 3.2.11, the remaining panels show the model results. Model output is shown at native grid to retain spatial detail.

[6] Data downloaded via KNMI Climate Explorer.

[7] https://gpm.nasa.gov/data/directory

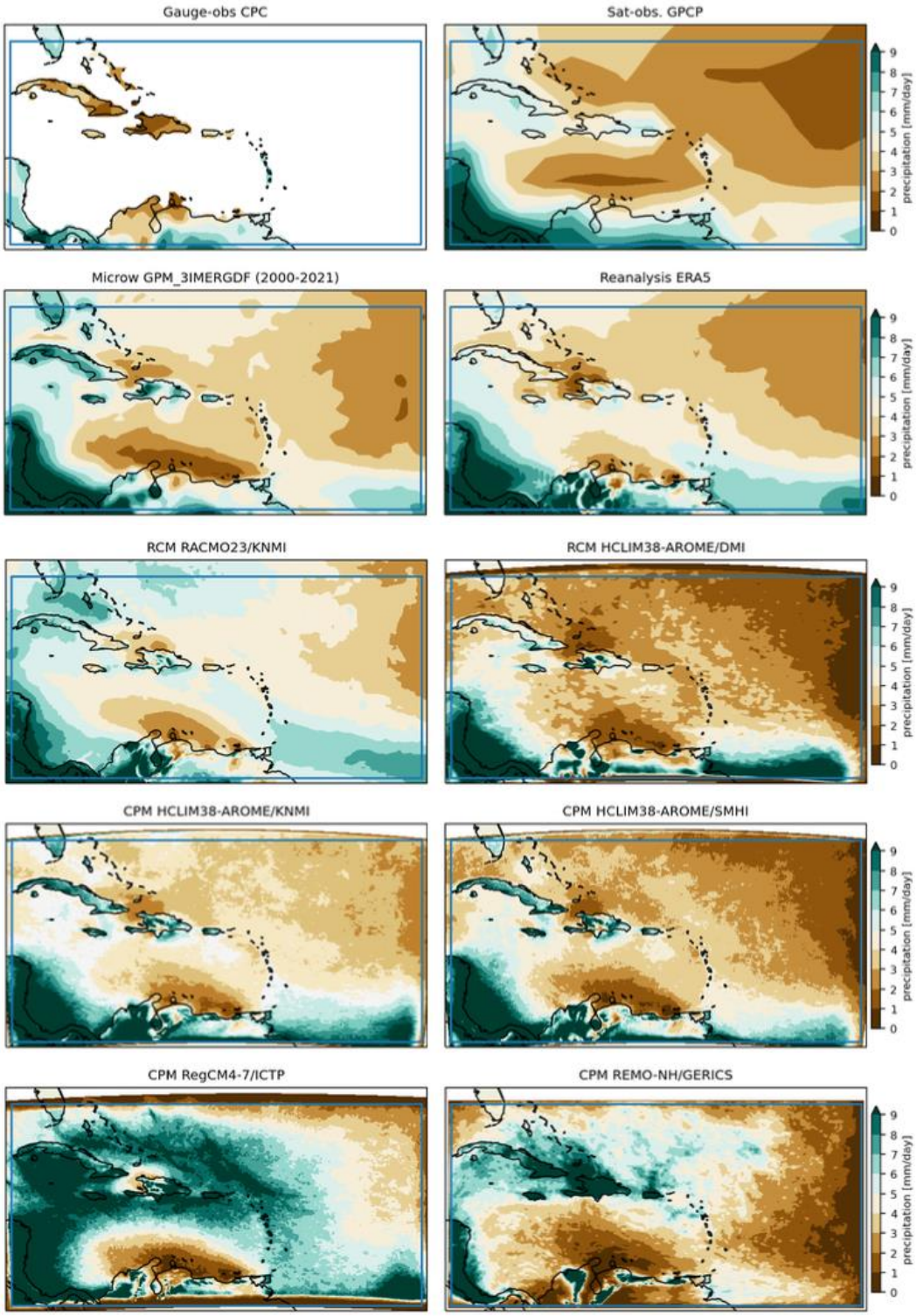

Fig 3.2.11: Mean precipitation (June-October), from observation records and ERA5 reanalysis (top two rows) and the RCM/CPM models (remaining rows). The blue box indicate the commonly agreed analysis domain.

There are sharp gradients in the precipitation pattern, both in the satellite observations, the reanalysis and all models. The eastern part of the domain is quite dry (generally a bit too dry in the models). (Sub-)tropical land areas and islands are wetter than the surrounding seas. Note that the rain-gauge based observations from CPC (top-left panel) do not agree with the other two observation sets over the large islands. The three HCLIM38-AROME variants (and also RACMO23 and the reanalysis ERA5)

have a pattern that is quite similar to the high-resolution observation set GPM. RegCM-4-7 is (much) wetter than the other models in most of the domain, especially in the west of the domain. In REMO-NH the large islands are particularly wet. If precipitation is split in wet-day frequency and intensity (using a wet-day threshold 1mm/day), it is found that the high average precipitation in the western part of RegCM-4-7 is mostly caused by a rather high wet-day frequency (not shown). In REMO-NH on the other hand, the wet-day intensity is very high.

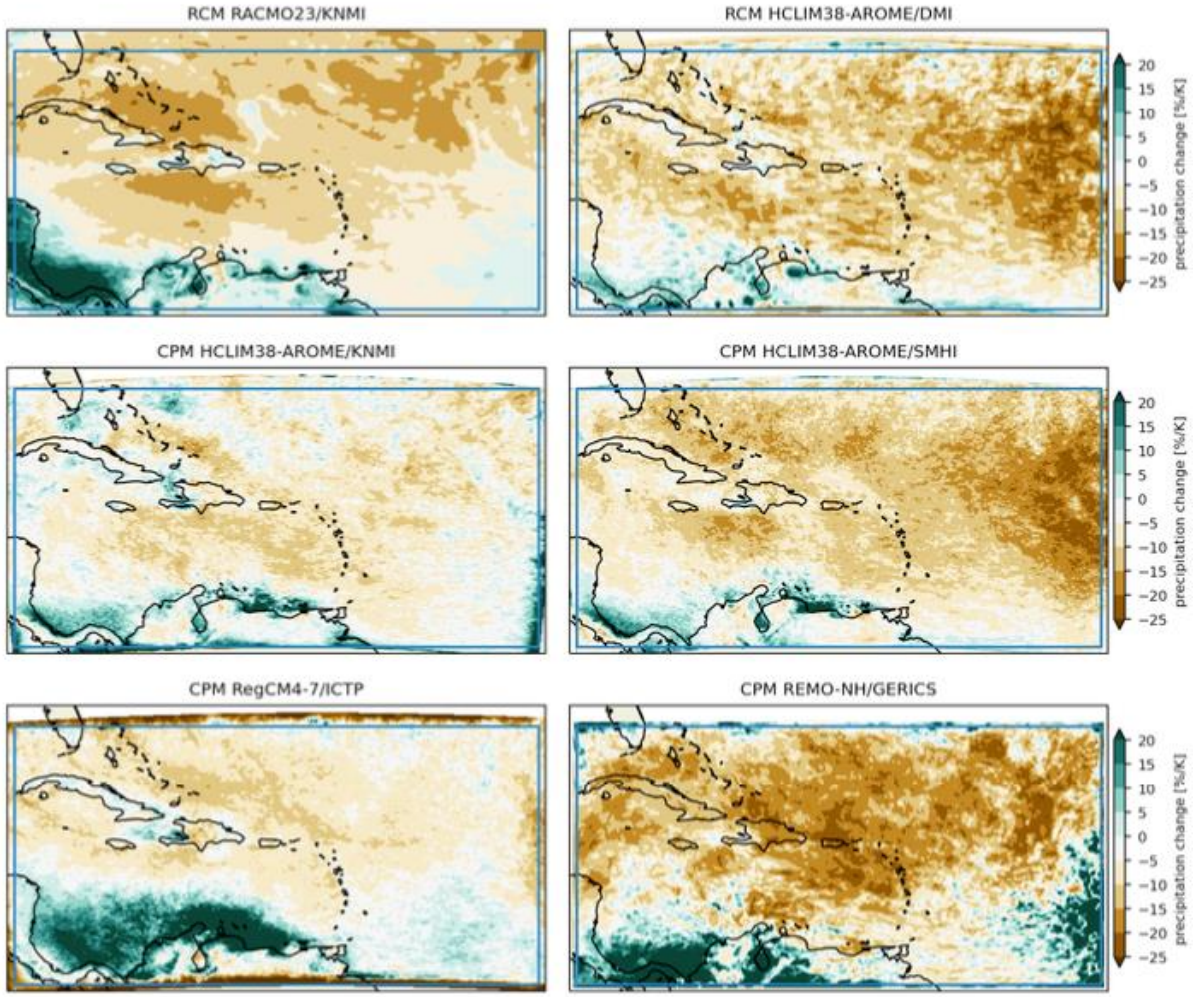

Fig 3.2.12: Future change in June-October average precipitation (in % per degree global warming, with dTglob = 3.38K), derived from the ERA5+PGW simulations.

Jones et al. (2016) provide an overview of precipitation trends in the region (see also Martinez et al. (2019) for an interesting review of precipitation mechanisms in the region). Using land observations taken from CRU and GPCC they found some positive (but hardly statistically significant) trends in precipitation over the largest islands (especially their western parts) during April-November. All regions however displayed significant decadal fluctuations in which systematically drier or wetter conditions persisted. PGW simulations have the advantage that they have a higher signal-to-noise ratio, because the future circulation conditions are approximately the same as in the current climate.

The future model changes are shown in Fig 3.2.12. A systematic drying signal emerges (mostly over sea) although on a local scale model spread and noise-levels are substantial. The net drying is caused by a reduction in the wet-day frequency (not shown), which in turn is likely related to the large-scale

changes (increased vertical stability, and reductions in mid-tropospheric relative humidity). Especially near land-sea borders and on the islands the model-spread is large. The increase seen in RegCM-4-7 and REMO-NH just north of the edge of the South-American continent is due to a strong increase in wet-day frequency. In RACMO23 on the other hand the increase in the south-western part is due to higher wet-day intensities. For completeness the ensemble-mean pattern of the future change (after conservative re-gridding to a common grid) is shown in Fig. 3.2.13. Crosses are used where the ensemble mean signal exceeds one ensemble standard deviation. The drying is reasonably robust, but this holds much less for the regions where precipitation increases.

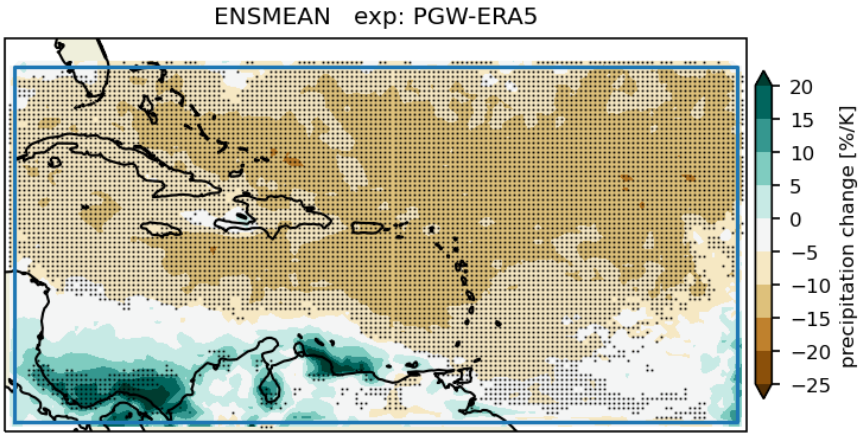

Fig 3.2.13: Ensemble-mean precipitation change. Dots are used to indicate regions where the ensemble mean change exceeds one ensemble standard deviation.

Precipitation extremes

We already noted the increase of the intense precipitation occurring in TC under PGW (and TP2 for RACMO2.3). Figure 3.2.14 shows the ensemble-mean response of daily and hourly precipitation extremes. To obtain these results, the model precipitation fields were first put on a regular 0.25x0.25 longitude-latitude grid (using conservative remapping). The pattern of the daily extremes (left panel) resembles the mean precipitation change, with a large region showing moderate decreases. For the hourly extremes (99%) the pattern is similar to the daily extremes (right panel). Only the highest local extremes (99.9% of the hourly values) show increases in a larger area of the domain. However, at this intensity the model spread in the responses is too large to have confidence in these pattern[8].

[8] Individual model results are available upon request at KNMI.

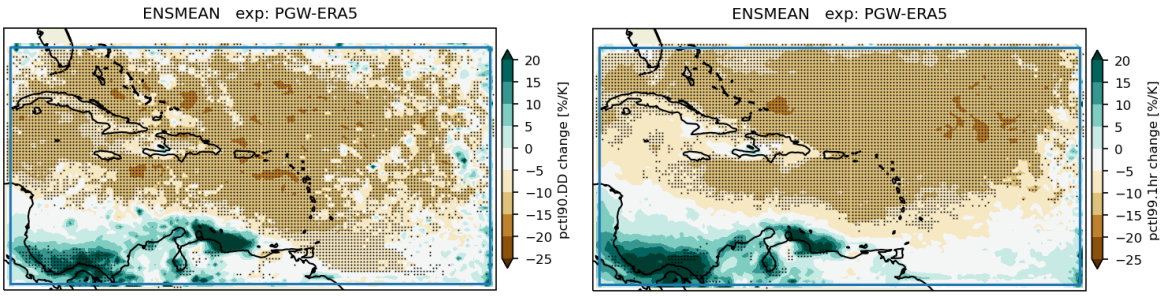

Figure 3.2.14: Future change of precipitation extremes. Left panel: 90% of daily precipitation; Right panel: 99% of the hourly precipitation. Data has been re-gridded to a regular 0.25x0.25 longitude/latitude grid prior to computation (conservative remapping). All models are included. Crosses are used where the ensemble-mean signal exceeds one ensemble standard-deviation.

Finally, we consider the *pooled fraction of exceedance*, computed by pooling data over the entire domain and over all seasons. Figure 3.2.15 shows the result for KNMI/HCLIM38-AROME (see suppl. figures for the other models). The black line gives the pooled fraction of exceedance of the REF simulation at a given hourly intensity (x-axis). The red line is the PGW result and the blue line the ratio PGW/REF. For HCLIM38-AROME the turning point is around 20mm/hour. Higher intensities occur more frequently under PGW, lower intensities occur less frequently. The ratio increases with increasing precipitation intensity. The grey shading shows that the scaling is ~7% per K warming for these higher intensities. Comparing this figure to Fig.3.2.12, we note that a substantial part of the increased precipitation extremes occurs in the south of the domain.

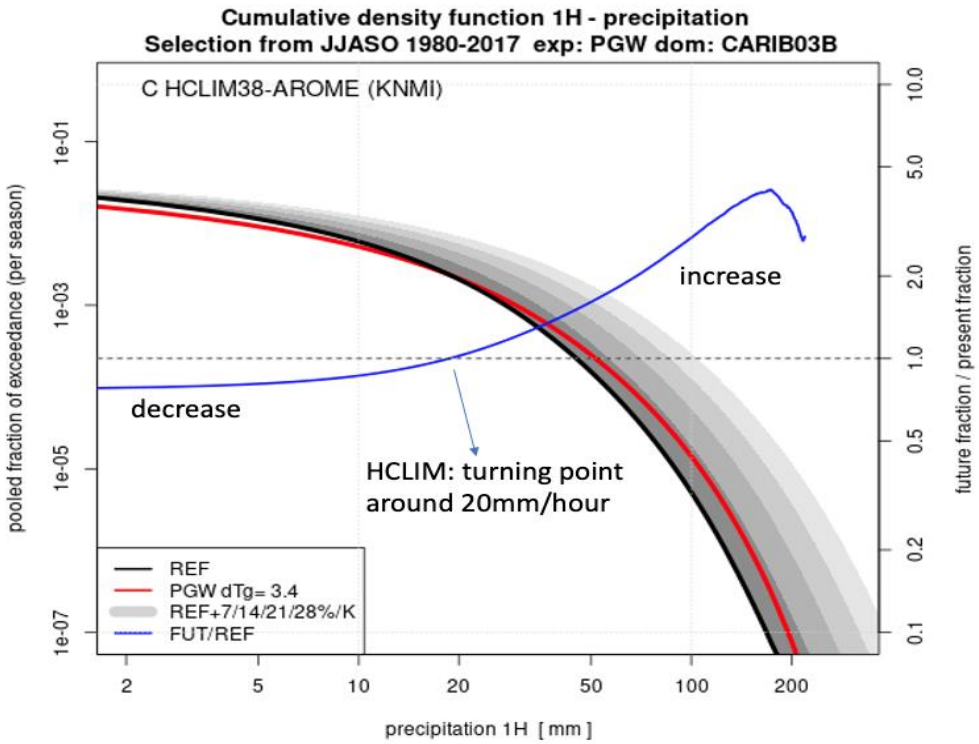

Figure 3.2.15: Hourly precipitation spatially and temporarily pooled over the entire domain. The black line denotes for each precipitation intensity (x-axis) the pooled fraction of exceedance in the REF run (y-axis). The red line shows the same for the PGW run. The blue line shows the ratio of the fractions. The grey-shading shows various scalings of the REF result with temperature.

Also, for precipitation there are substantial differences between the models. Especially the "turning-point" intensity (the intensity at which the ratio of the pooled fractions of exceedance becomes larger than 1) differs. The two HCLIM38-AROME versions (by KNMI and SMHI) are very similar. Again, the 12-km "low-resolution" convection-permitting version of HCLIM38 run by DMI produces results that are strikingly similar to those of the higher resolution version (SMHI). The other RCM (KNMI/RACMO2) on the other hand, produces systematically lower intensities. At the daily time-scale the qualitative picture does not change much (Supplemental figure S4) although quantitatively of course much higher values are obtained. For example, for KNMI/HCLIM38-AROME the daily "turning-point" is around 45mm, and precipitation intensities of 200mm/day (corresponding to a pooled fraction of exceedance of around 0.1% per season in the REF climate) are found ~2 times more frequently under PGW than in REF. A more complete analysis will be given in De Vries et al (*in preparation).*

3.2.4 Caribbean - Summary / outlook

In this chapter we have provided a first analysis of the pseudo-global warming simulations of the Caribbean conducted as part of EUCP. In total 6 models (4 CPMs and 2 RCMs) from 5 different groups contributed to this. To our knowledge this is the first time that such an endeavour has been undertaken. An evaluation of hurricane Irma provided some confidence that the models were able to resolve hurricanes, although considerable differences were found in the trajectories. This evaluation has been augmented with a subsequent analysis of the occurrences and changes of extreme wind speeds and by an TC-tracking analysis of one of the contributing simulations (RACMO). Furthermore, a multi-model analysis of precipitation, precipitation change and precipitation extremes has been given. Preliminary results have been presented at various EUCP meetings. In addition, an EUCP storyboard has been created for the Caribbean simulations to bring the results to potential end-users.

3.3 La Réunion

[main contributor: **CNRM**. Additional input from: KNMI]

3.3.1 Introduction

The island of La Réunion is a 2,512 km² island located in the Southwest Indian ocean at -21°05' N, 55°30'W. In total, about 860,000 inhabitants are living on this island resulting in a population density of about 340 inhabitants per square metre, close to that of a country like Belgium and greater than that of most large European countries (e.g., France, Germany, Spain, Italy, United Kingdom, etc.). A relevant characteristic of this island is its complex topography with its highest point reaching 3071 m. This complex orography has a great impact on the climatology of La Réunion resulting in a large spatial variability of both temperature and precipitation. Measured temperatures range from -5°C to 36.9°C and yearly precipitation accumulations range from 450 mm on the western side of the island up to 11000 mm on the eastern side. These extreme precipitation accumulations partially result from the combination of the steep orography and trade winds loaded with water vapour that condensate and precipitate when the air masses rise on the windward slopes. In addition, La Réunion is located in an area where tropical cyclones develop. When tropical cyclones hit La Réunion, it is often the first land they pass over. The steep orography they encounter results in world-record accumulations of precipitation with e.g., 1825 mm measured in 24 hours (in 1966) or 6083 mm in 15 days (in 1980).

With such extreme climatology in a densely-populated area, La Réunion is an important place to study and the Island's historical and future climates are of high scientific and societal interest. However, because of its small size compared to that of a typical GCM grid mesh, the island is not always represented in GCMs (i.e., it is most of the time replaced by sea). To address this issue, it is possible to downscale the GCM output dynamically. In collaboration with the CNRM, Meteo-France has carried out some simulations with the regional climate model (RCM) of Meteo-France ALADIN. In this simulation, the island appears to allow interaction with the atmosphere. Still, as shown in Fig. 3.3.1, the representation of the orography by CNRM-ALADIN is crude, and the realism of the interaction with the atmosphere is limited. The use of a model with a finer spatial resolution is needed for an improved representation of these processes (i.e., the interaction of the trade winds with the island).

The use of CNRM-AROME, the next generation of RCM used at the CNRM, shows a clear improvement in the description of the representation of the orography. In addition, the CNRM-AROME is a convection-permitting model and is likely to provide an important added value in the region of La Réunion island, where the fraction of convective precipitation over the total precipitation is above 70% (Gao et al., 2017). Finally, a large number of convective processes are taking place in tropical cyclones for which CPMs are also good candidates for providing added value. In this report, we will describe the method that is used to perform climate simulations using AROME at convection-permitting scale (section 3.3.2). In addition, we will very briefly review CNRM-AROME performance in representing precipitation over La Réunion and the projection for a single realisation (section 3.3.3). This report will only discuss a very small part of the potential of these simulations. We will, therefore, briefly describe how these simulations will be used in the future by our institute or the institutes that have already shown their interest in using these simulations (section 3.3.4).

3.3.2 Simulation description & Methods

The CNRM-AROME (Termonia et al., 2018; Fumière et al., 2019; Caillaud et al. 2021) simulations are performed based on a double nesting strategy. First, a CMIP6 simulation performed with the model CNRM-ESM2-1 (Seferian et al. 2019) output is used to force the CNRM-ALADIN model (Spiridonov et al., 2005; Déqué and Somot 2008) at its boundary. This model produces output at an hourly frequency and a spatial resolution of ~12 km. This output is then used as input for the CNRM-AROME simulations resulting in hourly output at a spatial resolution of ~2.5km. As shown in Fig. 3.3.1, the simulation domain of CNRM-AROME is not centred over the island of La Réunion. Instead, it is shifted toward the North-East as most of the air masses are entering the domain from this boundary. This allows for the different processes (e.g., cyclones) to develop before reaching the island of La Réunion.

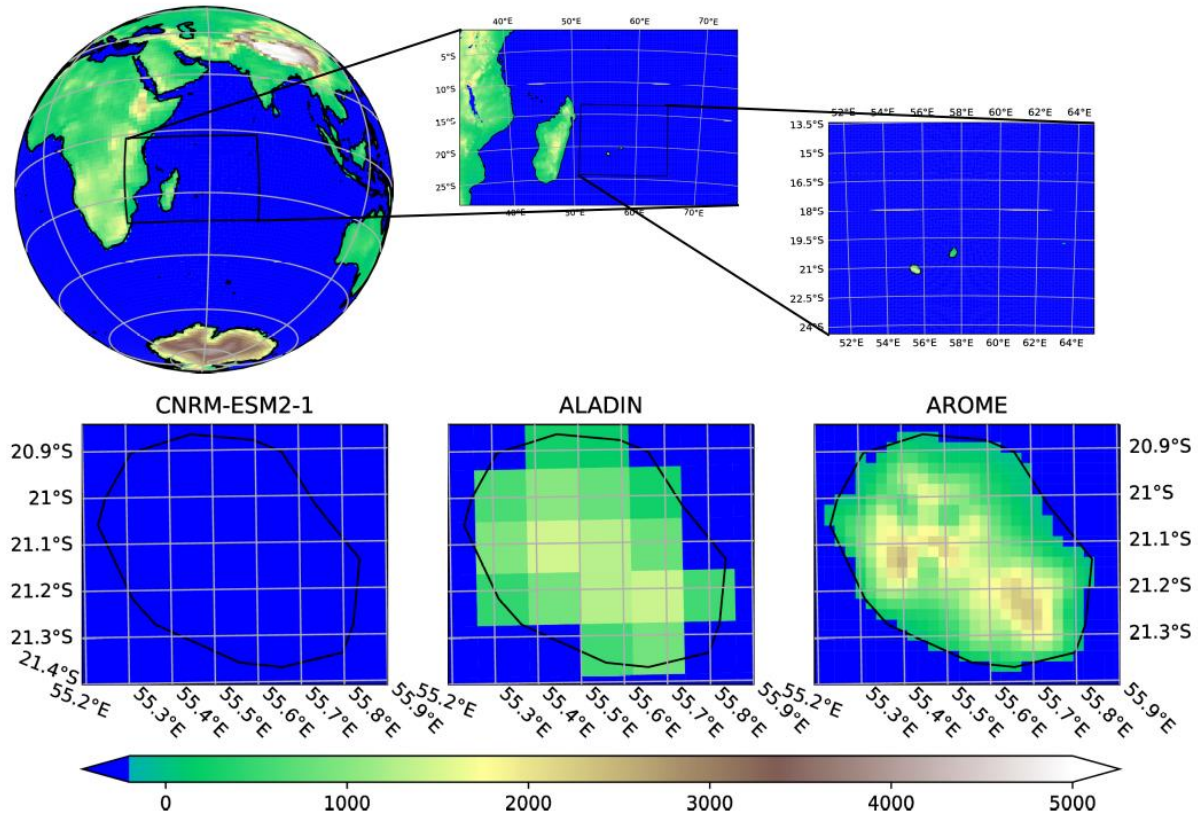

Fig. 3.3.1: Nesting strategy from CNRM-ESM2-1 to AROME. In addition, the different representations of orography for the different climate models used in this nesting strategy are shown.

While the CNRM-ESM2-1 and the CNRM-ALADIN simulations had already been performed, it was the first time that CNRM-AROME was applied to a tropical area as a climate model. Indeed, the CNRM-AROME had only been used over this area as a numerical weather prediction (NWP) model. Some technical work was performed to prepare the external datasets for this simulation. In addition, different tests were performed to investigate AROME robustness to the tropical climate. The number of vertical levels, as well as the hydrometeors diffusion parameters, were advised by the CNRM team working with AROME in NWP mode over La Reunion Island for being tested. None of these tests gave significantly better performance than the setup that is usually used when integrating AROME over the European continent. While such conclusions may be unexpected, it shows that AROME physics is robust, increasing our confidence that AROME is likely to also produce robust climate change signals. These tests were also used to ensure that the CNRM-AROME was able to represent tropical cyclones.

As shown in Fig. 3.3.2 (see Cyclone over "La Réunion" Island: AROME vs ALADIN vs CNRM-ESM2 for full video), tropical cyclones as simulated by AROME appear more realistic than those simulated by ALADIN, although no in-depth analyses were performed up to now on this topic.

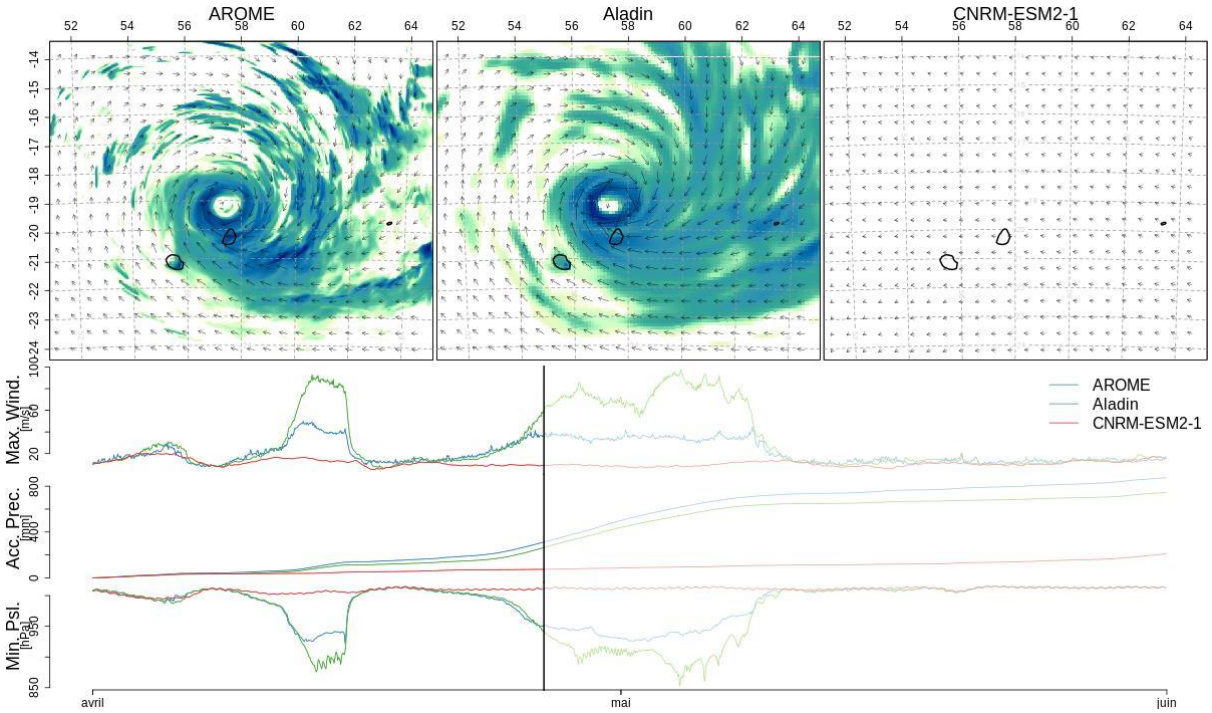

Fig. 3.3.2: Examples of Cyclones as represented by the CNRM AROME, the ALADIN and the CNRM-ESM2-1 models. The maps show hourly precipitation accumulations, while the lower part of the figure shows the maximum wind speed, the accumulated precipitation and the minimum sea-level pressure. The figure is part of a video that can be watched by clicking on the following link: Cyclone over "La Réunion" Island: AROME vs ALADIN vs CNRM-ESM2

Two simulations of 20-year long periods were produced over the domain shown in Fig. 3.3.1. The first simulation is based on the CNRM-ESM2-1 r1i1p1f2 historical simulation for the period 1991-2010. The second simulation is based on the CNRM-ESM2-1 r1i1p1f2 ssp585 CMIP6 simulation for the period 2081-2100. For each simulation a two-month spin-up period was performed at the beginning of the rainy season (i.e., November) to correctly initialise the soil moisture. These two-month periods are discarded from the analyses presented in this report.

For evaluating these simulations we use daily and hourly station-based observations from the Meteo-France observation network. A summary of the selected stations is shown in Fig. 3.3.3. These stations are selected based on the following criteria:

1. The station is located above a grid-point represented as land in the CNRM-AROME model.
2. The time series contains at least a ten-year period for the daily station or a five-year period for the hourly station.
3. These periods are not necessarily continuous in time, but each year selected has a maximum of 5% of missing data.

Both the accumulated precipitation and the two-metre temperature are extracted from these stations. Note that apart from these selection criteria, the quality of the measurements was not assessed for this report.

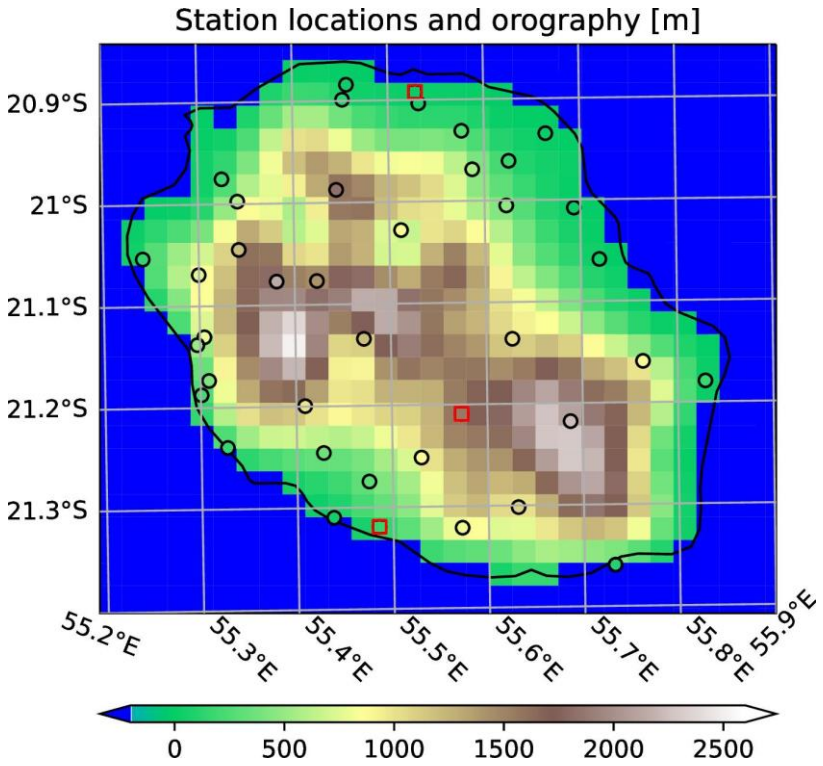

Fig. 3.3.3: Stations selected for the evaluation of the CNRM-AROME model. The orography as represented by the CNRM-AROME is shown as background colour and that of the stations are shown within the circle or the square. Black circles show stations providing daily measurements while red squares show stations with hourly measurements.

3.3.3 Results

In general, the two-metre temperature is well reproduced by CNRM-AROME (Fig. 3.3.4). The stations close to the coast at the lowest altitude are warmer than those at high altitudes as expected. Some stations located in areas with strong vertical gradients show the greatest biases. It is unknown whether this difference is related to the spatial resolution too coarse for representing the complex orography of the Island or to deficiencies of the AROME model in representing some physical processes such as those related to mountain breezes.

When comparing the two simulated periods, a clear warming signal is observed (Fig. 3.3.4). Over the island, this warming is 3.8 K, which is 0.5 K warmer than the warming as modelled by the CNRM-ESM2-1 simulations (Fig. 3.3.5). This warming is stronger over the island than over the sea and increases with altitude. It, notably, reaches 4.0 K for areas above 1000 metre and 4.4 K for areas above 2000 metre). In addition, on the Eastern coast, the warming is mitigated probably due to the trade winds that directly transport the air masses from the sea over this area. Finally, the warming is found to intensify for the warmest days, with, e.g., a 4.2 K warming for the 99th daily temperature percentile over the island (not shown).

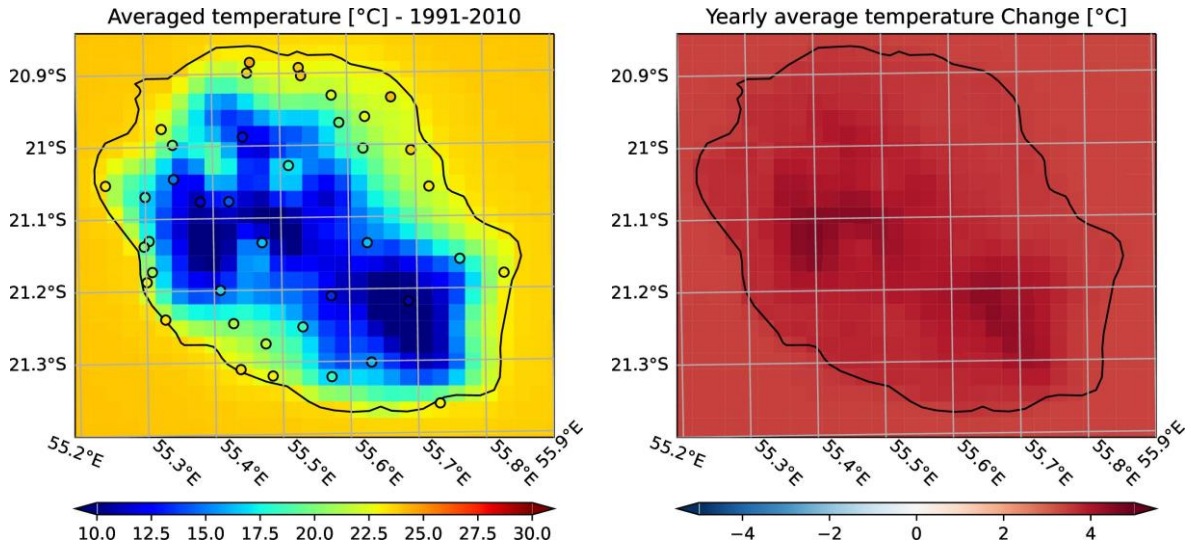

Fig 3.3.4: Averaged temperature as represented by the AROME model. On the left, the historical period is shown together with the observed values (circles). On the right, the difference between the two simulated periods (2081-2100 minus 1991-2010).

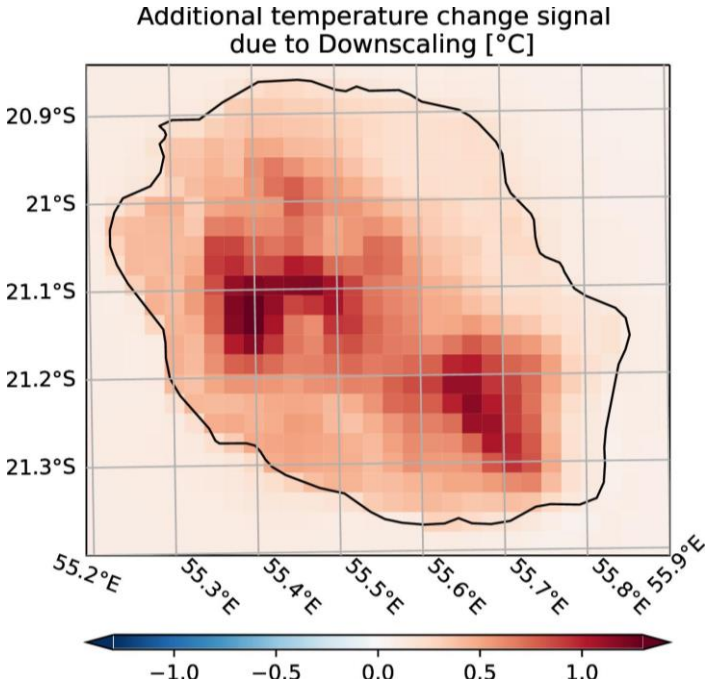

Fig. 3.3.5: Additional temperature change due to the dynamical downscaling. These values are derived by subtracting the temperature change as represented by CNRM-ESM2-1 from that of CNRM-AROME.

As opposed to the representation of temperature, the representation of precipitation suffers an important overestimation compared to the observed values (Fig. 3.3.6). Indeed, while the spatial pattern found in the observation, i.e., higher accumulation over the South-East than along the western coasts, is rather well reproduced by the CNRM-AROME, the accumulation is overestimated by more than 300% over the rainiest areas. Such overestimation is also found for the extremes as shown by the 99th daily precipitation percentile (Fig. 3.3.7) and the 99.9th hourly precipitation percentile (Fig. 3.3.8).

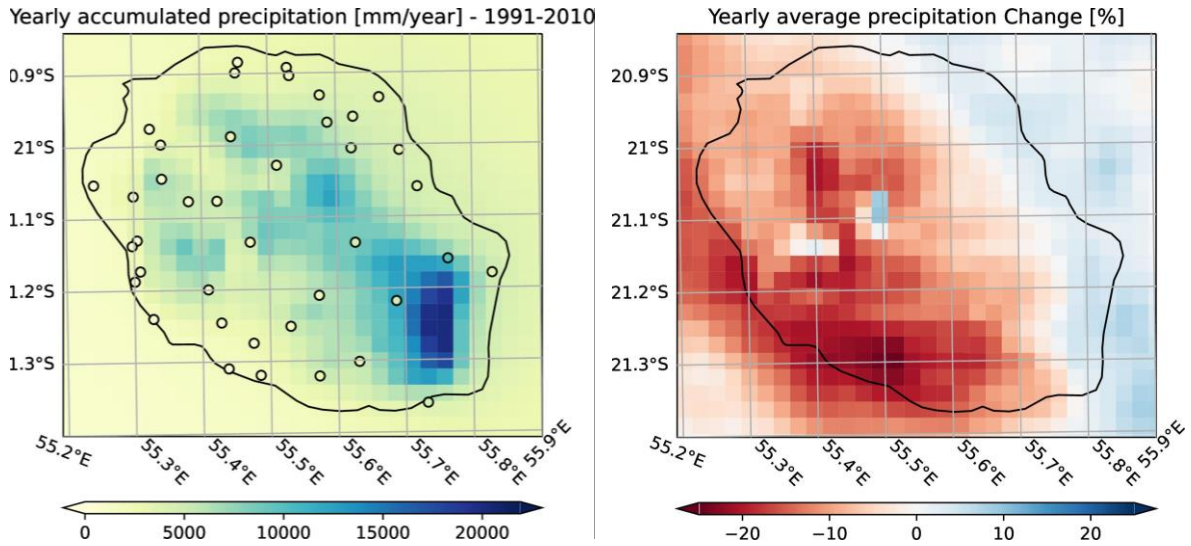

Fig 3.3.6: Averaged yearly accumulated precipitation as represented by the AROME model. On the left, the historical period is shown together with the observed values (circles). On the right, the difference between the two simulated periods (2081-2100 minus 1991-2010).

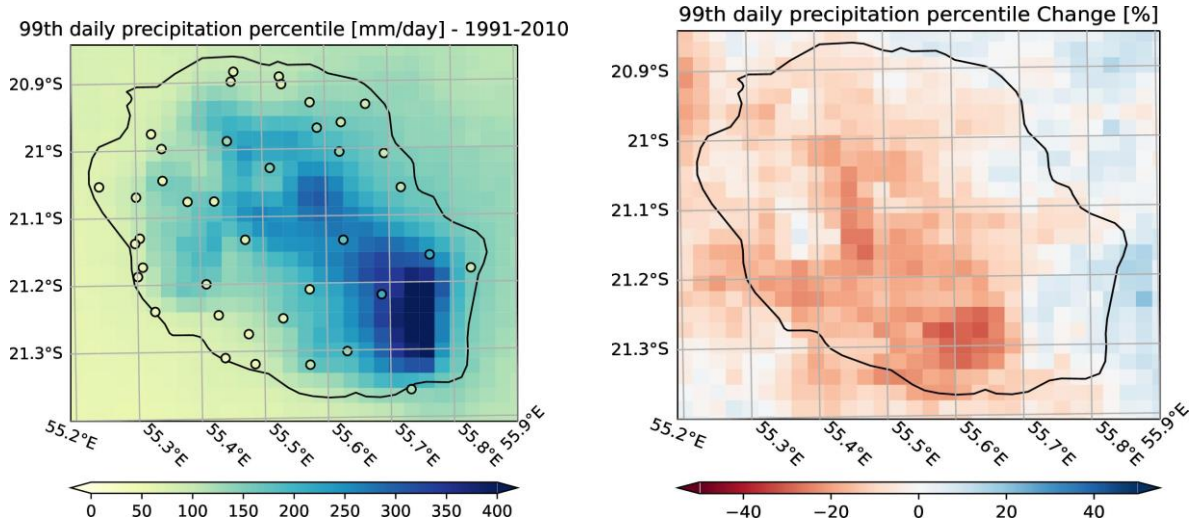

Fig 3.3.7: 99th daily precipitation percentile as represented by the AROME model. On the left, the historical period is shown together with the observed values (circles). On the right, the difference between the two simulated periods (2081-2100 minus 1991-2010).

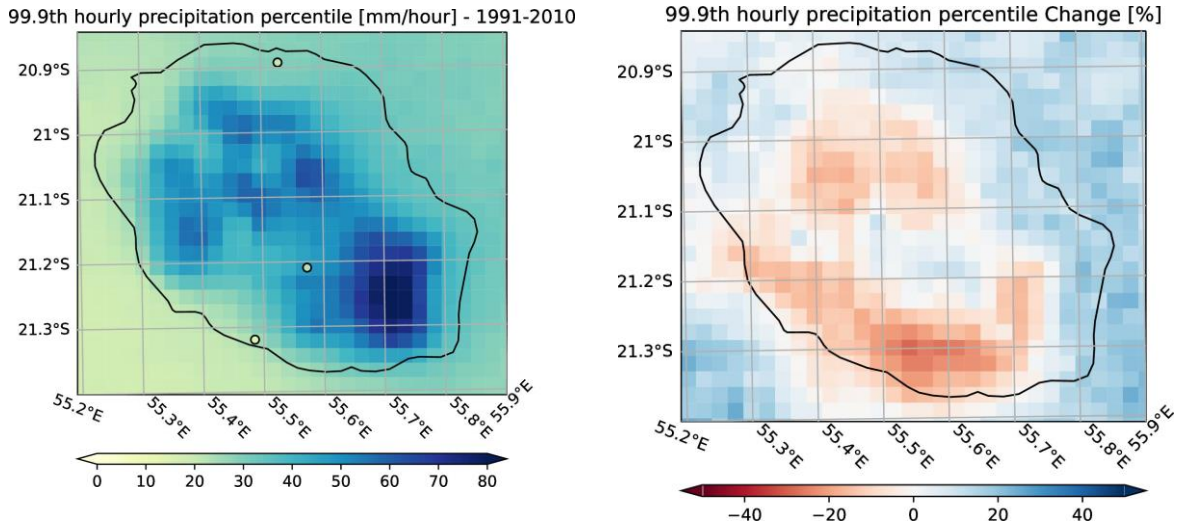

Fig 3.3.8: 99.9th hourly precipitation percentile as represented by the AROME model. On the left, the historical period is shown together with the observed values (circles). On the right the difference between the two simulated periods (2081-2100 minus 1991-2010).

This overestimation is higher during the wet season while it is moderate to non-existent during the dry months as shown in Fig. 3.3.9. The representation of the yearly cycle pattern is, therefore, too strong. Interestingly, the uncertainty shown by the ribbons in Fig. 3.3.9 is much larger for the wet months than for the dry months. This uncertainty reaches 110% of the monthly precipitation average in March against 45% for September. This difference may be explained by the large impact of tropical cyclones, rare events, which control a large part of the multi-year monthly values shown in Fig. 3.3.9. As this brief evaluation is performed using a historical simulation (as opposed to a re-analysis forced simulation), it is possible that the large differences seen between the observation and the model simulations are arising from driving conditions that are far from observed conditions (e.g., too many or too intense cyclones in the driving conditions than in the reality reflected by the observation). Further analyses that would notably assess the quality of the driving conditions are needed to understand whether CNRM-AROME is responsible for the strong overestimation of precipitation shown in this report.

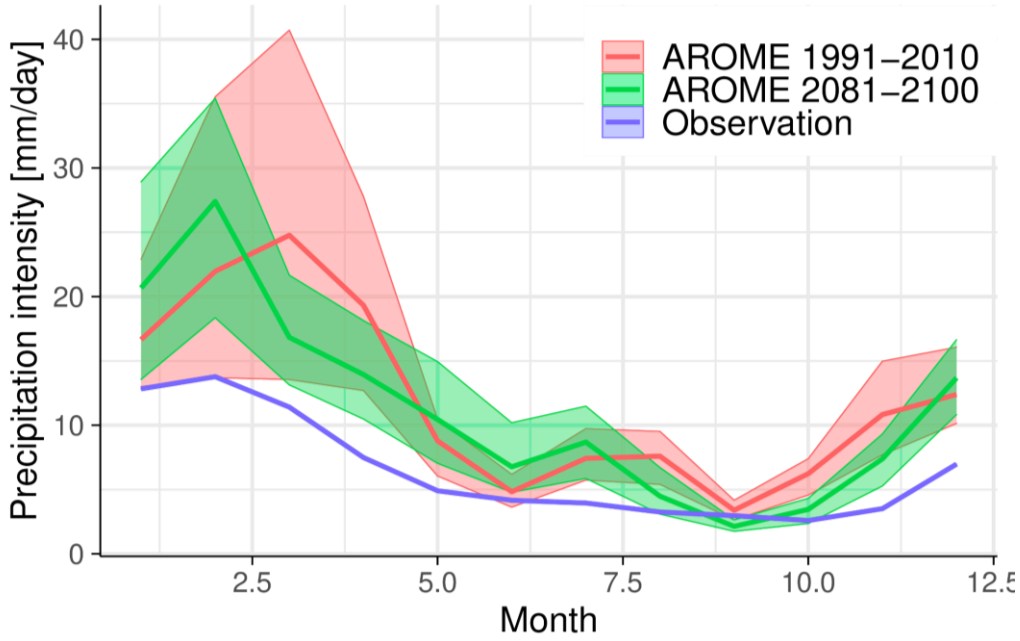

Fig. 3.3.9: Yearly cycle for both CNRM-AROME simulations (1991-2010 in red and 2081-2100 in green) and for the observations. For the model, the ribbons are derived by taking the range of the yearly cycle derived using 100 bootstraps with replacement with yearly blocks.

In general, the precipitation response to the global warming shown by CNRM-AROME consists of drying over most of the island except from its eastern side (Fig. 3.3.6). This pattern is also found for the 99th daily precipitation percentile (Fig. 3.3.7). Interestingly, the spatial pattern of the 99.9th hourly precipitation percentile differs over some areas of the island (Fig. 3.3.8). The yearly cycle shows an earlier precipitation maximum for the 2081-2100 period than for the 1991-2010 period. However, as explained in the previous paragraph, these diagnostics (i.e., mean, extremes or yearly cycles) may be largely impacted by the driving conditions and may, therefore, limit the conclusions of this analysis. Therefore, before concluding in a positive or negative response of precipitation due to global warming, it is needed to assess the relevance of the driving conditions used as input to the CNRM AROME model. More simulations or other methods, not developed in this brief report (e.g., combinations of dynamical/statistical methods or comparisons to the driving conditions), are needed to robustly assess the impact of global warming on La Réunion Island climate.

3.3.4 la Réunion - Summary / outlook

A set of convection-permitting climate simulations were performed over La Réunion Island for the very first time with the CNRM-AROME regional climate model. This set of simulations consists of two 20-year experiments that use the CMIP6 simulations derived from CNRM-ESM2-1 and the CNRM-ALADIN as boundary conditions. The temperatures represented by the historical simulation (1991-2010) are close to the observations while precipitation is severely overestimated.

The second simulation follows the SSP585 for the period 2081-2100. Using these simulations, an important warming-signal is found over the island. This signal is stronger in CNRM-AROME compared to that of CNRM-ESM2-1, probably due to a more realistic representation of the surface in CNRM-AROME. In this simulation the mean precipitation and the largest daily accumulations decrease over most of the island, except over its eastern side.

The interannual variability shows an important sensitivity of precipitation to large-scale conditions. It is unknown whether this sensitivity explains the overestimation of precipitation by the CNRM-AROME or if the differences arise from deficiencies in the CNRM-AROME. This sensitivity limits the conclusions of the model evaluation and may impact the analysis of the precipitation response to global warming. Further studies are needed to understand the impact of this sensitivity. Such studies are likely to be carried out in the near future. Indeed, these simulations have already been shared with scientific groups in and outside of the CNRM. These groups are notably currently investigating the added-value of performing convection-permitting simulations over tropical Islands. In addition, it is planned to track tropical cyclones to create composites and compare those to similar products derived from CNRM-ALADIN and CNRM-ESM2-1. Finally, it is planned to either use these simulations as they are or to use these simulations for assessing CNRM-AROME deficiencies, then adjust the model setup before performing further simulations.

3.4 Canary Islands and Madeira

[main contributor: **CMCC & ETH**. Additional input from: KNMI]

3.4.1 Introduction

The extreme events and dynamical effects over Canary islands and Madeira were explored with the EU's outermost regional climate simulations developed in the context of the EUCP project. According to UNESCO (Falkland and Custodio 1991), island environments that are smaller than 2000 km^2 or have a maximum width smaller than 10 km can be categorised as small islands. This is the case for Canary islands and Madeira that still host more than 2,1M people (Madruga et al. 2016) and provide important ecosystem services due to their unique landscapes, as well as strategic and economic benefits to their countries. Nonetheless, due to their geographical position, Canary islands and Madeira are not included in European ensemble climate simulations as the ones over the EURO-CORDEX domain. In order to cover the gap, within the EUCP project, we examine future changes in precipitation events and the development of vortex streets of mountainous islands within the context of very high-resolution regional climate modelling. The relevance of phenomena such as extreme events and dynamical effects over Madeira island was also highlighted in literature (Schär and Durran 1997, Fragoso et al. 2012).

In general, extreme events of precipitation are of interest both to scientists and decision makers because of their potential to cause considerable damage and impacts on people, infrastructure, and the environment. In order to provide a proper characterization of extremes, address hazard assessment and manage associated risk, an increasing number of studies show improvements in regional climate model performances at a very high-resolution scale. Such improvements have been exploited especially over complex orography (e.g., the Alps) by using convection permitting models. The complex orography of small islands, such as Canary and Madeira, favours the creation of microclimates, which was not yet studied using convection permitting models and cannot be studied using conventional global or regional climate models with moderate resolution. Previous studies on such territories use regional models at a resolution of at least a few kilometres to reproduce the observed geographical distribution of temperature and, especially, precipitation (Pérez et al. 2014, Expósito et al. 2015).

3.4.2 Simulation description & methods

Two groups participated in the simulations for the Canary islands and Madeira (details in table 3.4.1 below). CMCC adopted a time-slice approach while ETHZ adopted the Pseudo Global Warming (PGW) approach. In this report the future PGW simulations by ETHZ are not discussed as time constraints and staff changes did not allow the required analysis to be performed. The data is however available upon request.

Table 3.4.1: Details of groups participating in simulations for Canary islands and Madeira.

Group	Model	RCM/CPM	Resolution	Details
CMCC	COSMO-CLM v5.09	CPM	~3km	Triple nesting (GCM EC-EARTH – 0.44° CCLM – 0.22° CCLM) and time slice approach
ETHZ	COSMO-crCLIM	CPM	1.1 km	Two-step one-way nesting at 12 km and 1.1 km using ERA-Interim boundary conditions.

CMCC simulation strategy and method

The GCM-driven simulations have been completed by CMCC using continuous simulations of 10 years with a time slice approach. The simulations are developed with the regional climate model COSMO-CLM (version 5.00 clm9) in convection-permitting mode. More specifically, the driving data provided by the global climate model EC-EARTH (realisation 12) are downscaled first at an intermediate resolution of 0.44° (around 50 km) and then at 0.22° (around 25 km) over the MENA-CORDEX domain (Bucchignani et al. 2018). Then, a further downscaling at 0.0275° (around 3 km), nested into the previous one, is performed over a domain that includes Canary islands and Madeira (Fig. 3.4.1). A historical period (1996-2005) and a far future period (2090-2099) under IPCC RCP8.5 scenario have been considered.

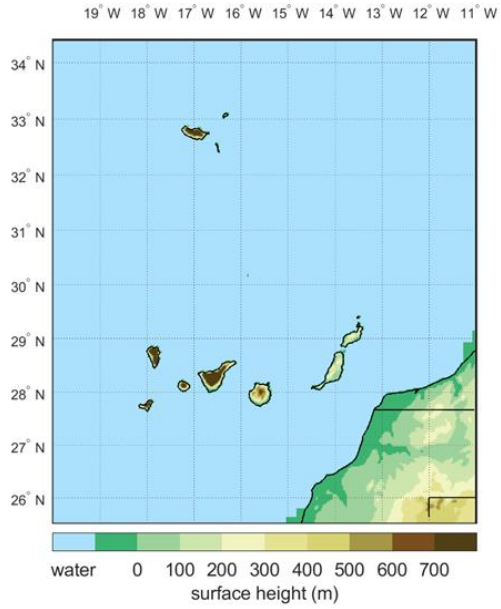

Figure 3.4.1: CMCC COSMO-CLM computational domain

Some further details are listed:

- Computational Domain: Canary Islands and Madeira (11°W – 20°W, 25.52°N – 34.4°N) with Nx=327, Ny=323, Nz=65
- Resolution: 0.0275°, ~3 km
- Sponge zone: 23 grid points

- Forcing data: two intermediate COSMO-CLM simulations over MENA-CORDEX domain at spatial resolutions of 0.44° and 0.22° driven by GCM EC-EARTH r12
- Experiments: - Historical 1996-2005 (1995 spin-up) - Far future 2090-2099 (2089 spin-up) scenario RCP8.5

The characteristics of precipitation and extremes are seasonally investigated at hourly scale in historical and far future experiments. The indicators assumed for the analysis are wet-hour frequency, wet-hour intensity and heavy precipitation assessed from the hourly precipitation. A wet hour is defined as an hour with precipitation greater or equal than 0.1mm (Ban et al., 2021). Heavy precipitation events are represented by the amount of hourly precipitation above a fixed percentile (99.9th) computed from all data (wet and dry events). Although 10-year simulations do not represent a sufficiently long period to identify climatological trends, the changes in such indicators are assessed in order to provide preliminary indications about the expected variations in future precipitation projections.

ETH simulation strategy and method

ETH uses the COSMO-crCLIM model. It is based on a version of the COSMO model that runs on Graphics Processing Units and exploits a Domain Specific Language. The implementation allows climate simulations over large domains at a reasonable cost (Leutwyler et al. 2017). The simulations over the Macaronesian domain use a two-step one-way nesting approach at 12 km grid spacing for the outer domain, in which convection is parameterized, and 1.1 km grid spacing for the inner domain, in which the convection scheme is switched off (Fig. 3.4.2). The 12 km simulations are driven by 6-hourly ERA-Interim reanalysis for the period 01/2000-12/2015. This includes a 5-year period for soil moisture spinup. The 1.1 km simulations are then conducted for the period 11/2005-12/2015, which includes a 2-month soil moisture spinup. The analysis period is 01/2006-12/2015. The future climate simulations use the Pseudo-Global Warming (PGW) approach (Brogli et al. 2019) with the change signal from MPI-ESM-LR RCP8.5 simulation. More specifically:

- Computational Domain: Canary Islands and Madeira (20.10°W – 13.5°W, 23.15°N – 35.85°N) with Nx=1000, Ny=1000, Nz=60
- Resolution: 0.01°, ~1.1 km
- Sponge zone: 30 grid points
- Forcing data: an intermediate COSMO-crCLIM simulation over a larger domain at spatial resolution of 0.11° driven by ERA-Interim
- Experiments: (i) Evaluation 2006-2015; (ii) PGW Far future scenario RCP8.5 – Signal from MPI-ESM-LR r1i1p1

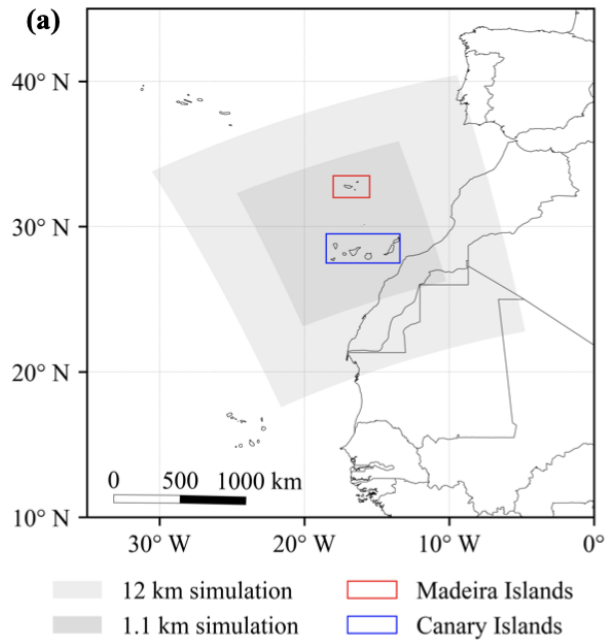

Figure 3.4.2: ETH COSMO-crCLIM computational domains at 12 km (light grey zone) and 1.1 km (dark grey zone) grid spacings. The location of Madeira and Canary Archipelagos are shown in the red and blue rectangles, respectively.

3.4.3 Results

3.4.3.1 Characteristics of precipitation and extremes (CMCC)

Following the aforementioned method based on hourly indicators of precipitation (Section 3.4.2), the results from CMCC simulations are presented in the following. Figure 3.4.3 refers to the historical period (1996-2005) and represents a reference for the changes shown in Figure 3.4.4. The future projections (2090-2099) compared with the present-day (1996-2005) simulation indicate a significant decrease of the hourly heavy precipitation (99.9th percentile) during the winter season (DJF) over almost the whole domain (Fig. 3.4.4). Such decrease is less pronounced during the spring (MAM) and summer (JJA) seasons although, during MAM, it still persists over Madeira and Tenerife islands. The autumn (SON) season is characterised by a decrease of the hourly heavy precipitation over Tenerife island and an increase over Madeira island. A slight decrease of the hourly intensity is projected in DJF, MAM and SON (except for the North part of the domain including Madeira island) while an increase is projected in JJA over almost the whole domain. A general reduction of hourly frequency is projected for DJF (with a north-south gradient) and MAM. A less significant reduction is projected for JJA and SON (except for Fuerteventura and Lanzarote islands) for the future period (2090-2099) with respect to the historical period (1996–2005).

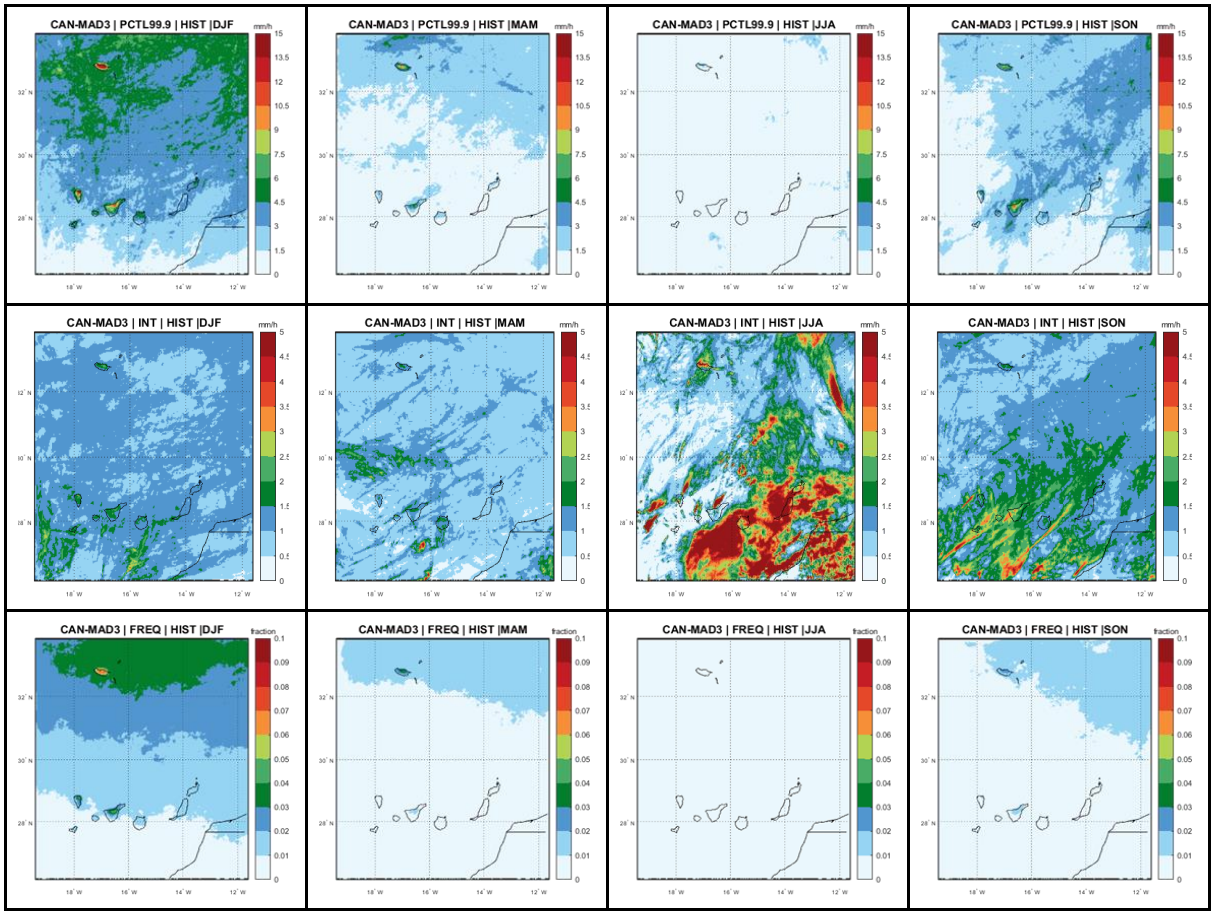

Figure 3.4.3: Reference maps from the historical period (1996–2005) of heavy precipitation (99.9th percentile), intensity and frequency at hourly scale in all seasons.

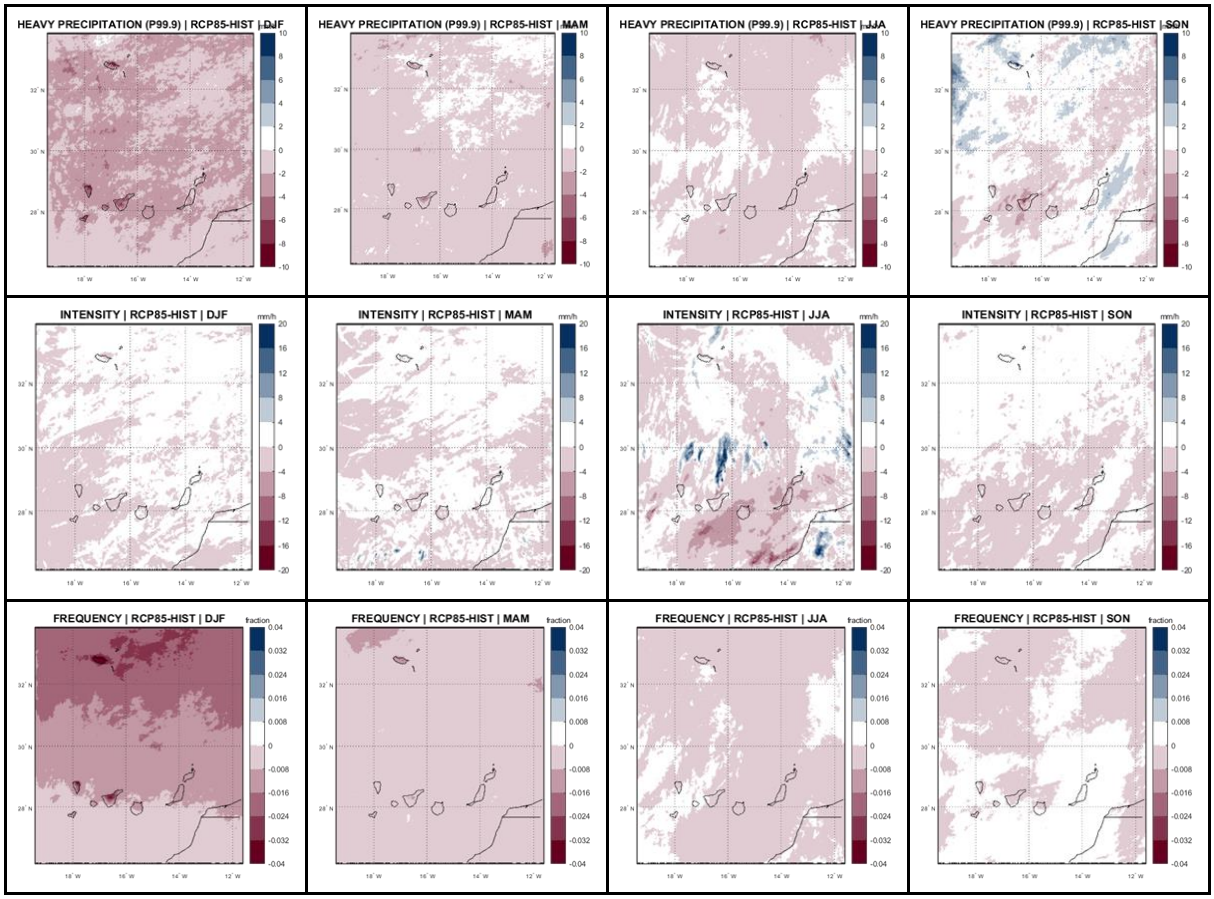

Figure 3.4.4: Changes in heavy precipitation (99.9th percentile), intensity and frequency at hourly scale in all seasons projected at the end of century (2090–2099) with respect to the historical period (1996–2005).

In order to have a statistical overview, Figure 3.4.5 represents the box plots of the changes in extreme precipitation events over Tenerife and Madeira islands. Tenerife island is characterised in far future projections by a general decrease in terms of heavy precipitation in all seasons except in JJA, when null variations are projected. Such change is associated with a decrease in frequency more pronounced in DJF and negligible in other seasons and a decrease in intensity that is almost uniform across seasons with a slight increase in the extreme intensities, especially during JJA. Madeira island is characterised by changes projected in the far future much more evident than the ones over Tenerife island in SON by an increase of hourly heavy precipitation with a reduction of frequency and an increase of intensity. In other seasons, a decrease of hourly heavy precipitation with a decrease in frequency but partial increase in intensity are projected for the end of the century.

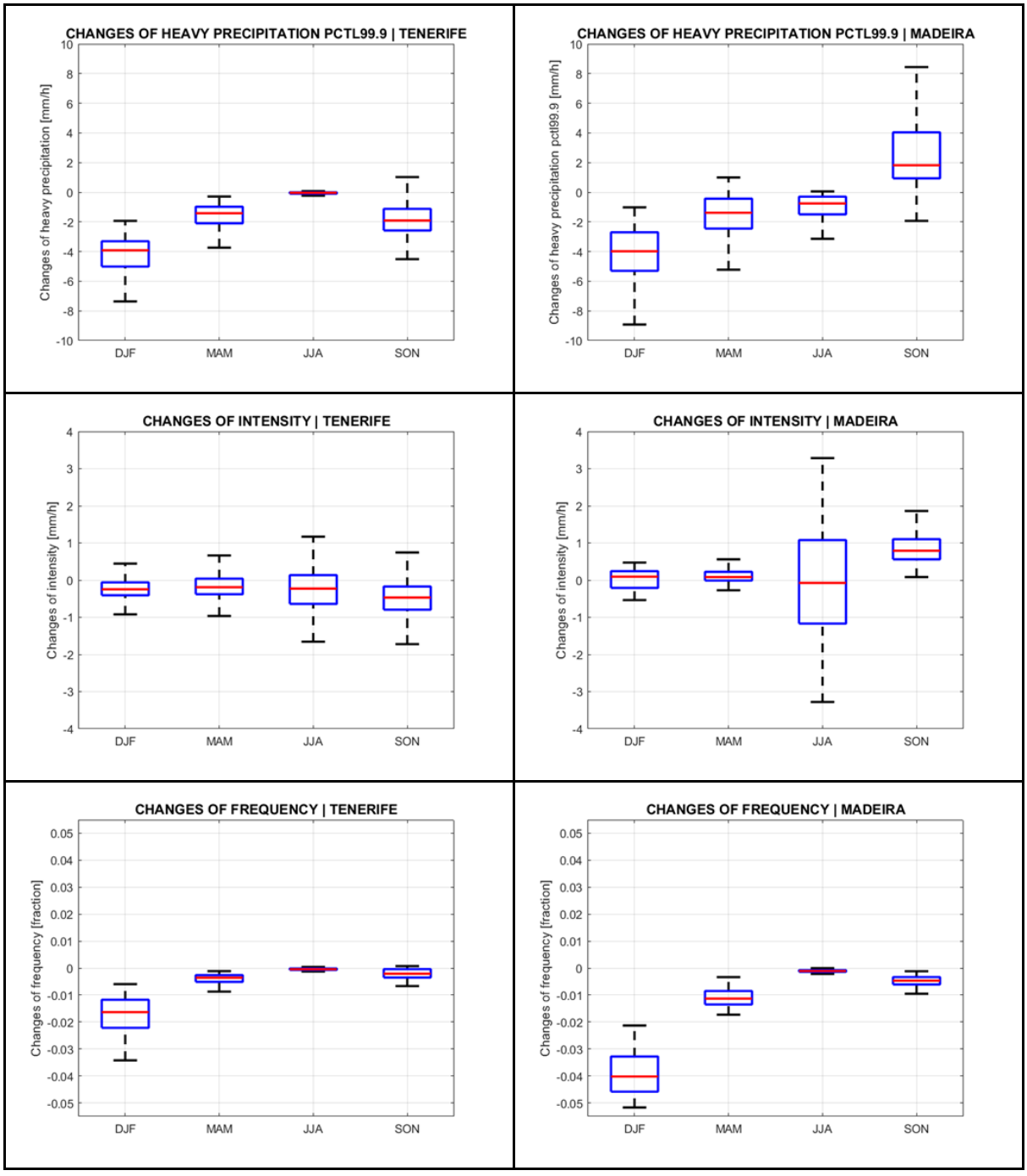

Figure 3.4.5: Box plots of changes in extreme precipitation events over Tenerife and Madeira islands.

3.4.3.2 Identification of vortex streets in the lee of Madeira (ETH)

[This section is based on the following paper in preparation: Gao et al. Vortex streets to the lee of Madeira in a km-resolution regional climate model.]

Flow around isolated mountainous islands can lead to the formation of atmospheric vortex streets. Atmospheric vortex streets are one of the widely studied dynamical effects of isolated islands. However, the study of vortex shedding is still limited by the availability of observational wind fields of high spatial and temporal resolutions and confined to case studies or idealised simulations. In this

study, we developed an algorithm that is able to identify vortex streets in convection permitting simulations. The algorithm is based on a wavelet analysis. Several criteria for identifying a vortex street in a grid cell are considered, such as a minimum value for relative vorticity of 3.10^{-4} s^{-1} and a minimum peak value of 4.10^{-4} s^{-1}, a minimum size of 100 km^2 to differentiate vortex streets from noise, as well as other criteria based on the shape, location, direction and duration of the vortex. We apply this algorithm on Madeira island to generate a climatology of vortex streets and shedding using the 1.1 km decadal simulation of COSMO-crCLIM (Section 3.4.2, red rectangle of Fig. 3.4.2).

The Madeira island is located near the north-western African coast and forms a part of Macaronesia, whose weather and climatic patterns are mainly influenced by the subtropical semi-permanent Azores high-pressure system. Madeira island is the largest (740 km^2) and highest (1862 m altitude) island in this archipelago and represents a major source of atmospheric flow disturbances. Due to its particular topography and location, Madeira is vulnerable to extreme weather events (Fragoso et al. 2012), such as the 20 February 2010 flash flood and mudslide that led to 51 deaths.

Madeira Island is characterised by more (less) precipitation in winter (summer) due to the southward (northward) migration of the Intertropical Convergence Zone and eastward (westward) movement of a precipitation region over the northwest Atlantic. More precipitation is observed in the north or northeast windward regions than in the lee sides due to prevailing north-easterlies and orographic lifting. Figure 3.4.6 shows annual mean precipitation over the Macaronesian domain and the Madeira island for the period 2006-2015. The annual precipitation ranges from 43 to 564 mm in ERA5 reanalysis over the whole domain (Fig. 3.4.6 a). Wetter conditions can be observed near or on the islands due to orographic lifting, which is especially noticeable over Madeira Island. Compared to reanalyses, the model is drier overall at both 12 km (Fig. 3.4.6 b) and 1 km (Fig. 3.4.6 c) grid spacings. However, the spatial patterns are well simulated, particularly at 1 km grid spacing. When zooming in on the Madeira Archipelago (Fig. 3.4.6 d-f), we notice that only the 1 km simulation is able to simulate the location of precipitation due to its more realistic topography. ERA5 is too coarse (0.25° horizontal grid spacing) to reveal precipitation patterns over Madeira Island, and the 12 km model wrongly simulates precipitation patterns in the lee of the island, which is attributed to its poorly resolved topography.

The vortex identification algorithm was validated using several case studies, such as the positive and negative vortices represented in Figure 3.4.7. This shows the ability of the model to simulate vortex sheddings of the Madeira island so it is possible to apply the algorithm on a decadal simulation.

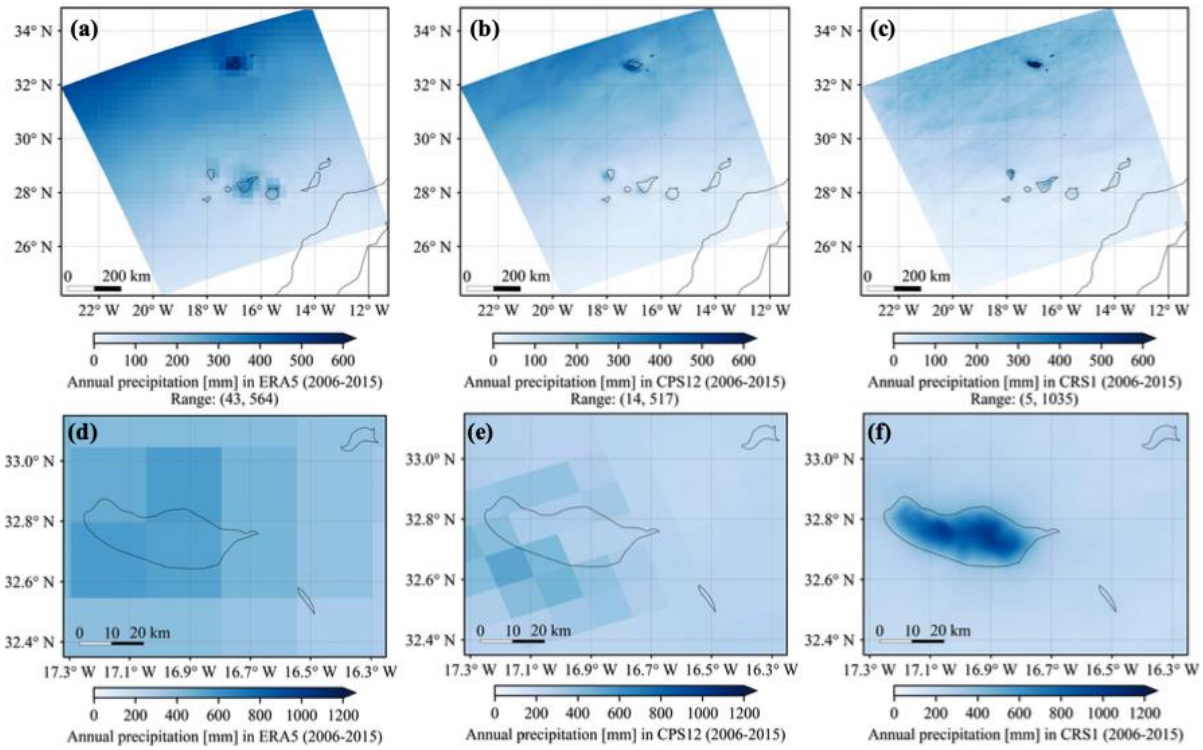

Figure 3.4.6: Annual mean precipitation [mm] over the analysis region (a-c) and Madeira Archipelago (d-f) in the ERA5 reanalysis (a and d), 12 km convection parameterized simulation (CPS12; b and e), and 1.1 km convection resolving simulation (CRS1; c and f) for the period 2006-2015. Please note the different scales for the top and bottom row panels.

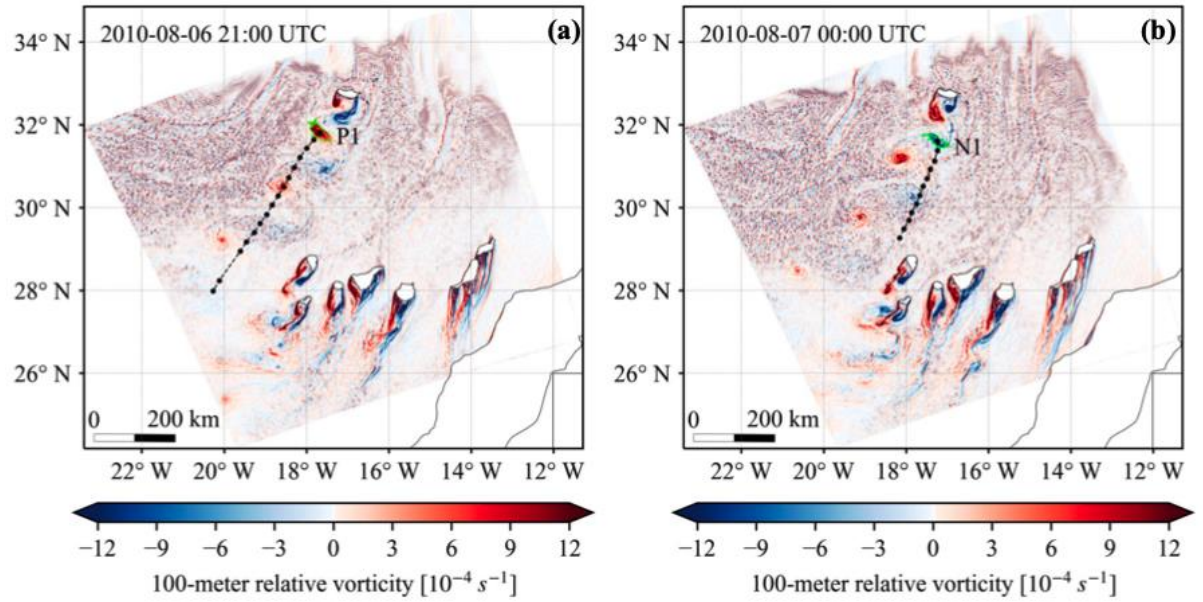

Figure 3.4.7: Tracks of vortex streets in the lee of Madeira Island. Black dots show hourly tracks for (a) a positive vortex (P1) shedded at 2010-08-06 21:00 UTC and (b) a negative vortex (N1) shedded at 2010-08-07 00:00 UTC. Colour shadings represent relative vorticity at 100m height [10^{-4} s^{-1}]. Black contours denote the islands of the 1 km Macaronesian domain.

Figure 3.4.8 shows the number of vortices that were identified on each grid point by the algorithm. Over a total of 87,648 simulated hours that correspond to the 2006-2015 period of the decadal simulation, a maximum of 1097 vortices on a single grid cell were identified. Vortices shedded from Madeira Island mainly propagate in the south-west direction because of prevailing north-easterlies, which is consistent with the case study simulations.

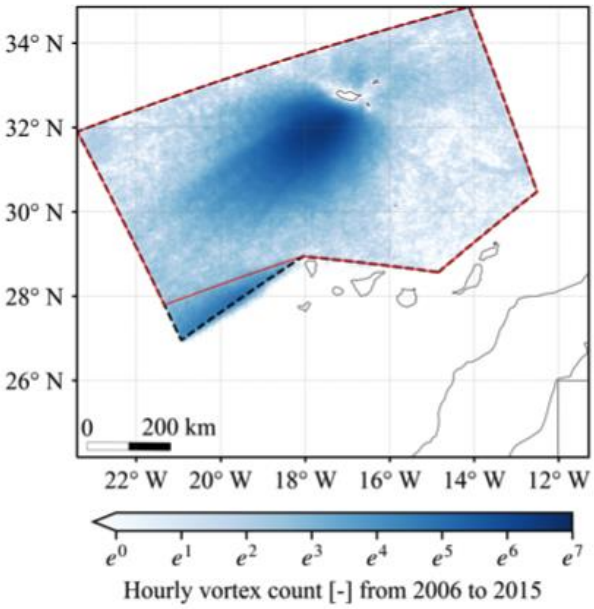

Figure 3.4.8: Count of simulated vortices every hour at each grid cell from 2006 to 2015 over the dashed black polygon. The exponential scale is used to account for the unevenly distributed vortices. The red polygon is used for identifying vortices at the lee of Madeira to avoid vortices shedded from La Palma island in Canary Archipelago.

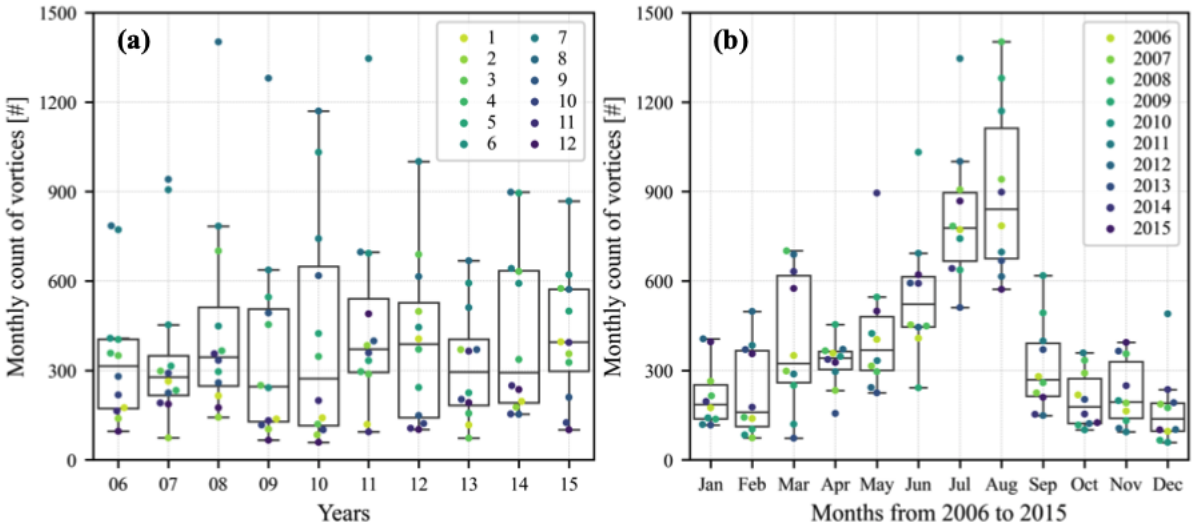

Figure 3.4.9: Boxplot of the monthly count of identified simulated vortices (a) in each year from 2006 to 2015 and (b) in each month. The boxes show quartiles of the data, and the whiskers extend to values within 1.5 times of the inter-quartile range from the low or high quartiles.

The interannual variability of the number of vortices is large with a median count of about 300 vortex shedding per month but a maximum number that can reach about 1400 vortices (Fig. 3.4.9 a). The annual cycle is large as well, with a minimum in December and January, a gradual increase from spring to summer, and a maximum in August (Fig. 3.4.9 b). This is explained by increasing wind speed in the south-west direction from March to August, which suddenly decelerates in September, resulting in less vortex sheddings (not shown). This result is consistent with Grubišić et al. (2015) based on satellite observations. The monthly variability in vortex shedding is attributed to the migration of the Hadley

circulation (Carrillo et al. 2016). The location, shape and magnitude of the Azores High also influence vortex shedding in the lee of Madeira Island (not shown).

3.4.4 Canary Island and Madeira - Summary / outlook

The island of Madeira was hit by several extreme events of precipitations that triggered catastrophic flash-floods. Fragoso et al. (2012) report an overview of the main flash-flood events in Madeira between 1800 and 2010. Moreover, a strong relationship between the North Atlantic oscillation (NAO) and rainfall changes has been observed at southern slopes of the western Canary Islands in the same seasons (Herrera et al. 2001). The NAO is the dominant mode of winter climate variability in the North Atlantic area on monthly to decadal timescales particularly associated with rainfall variability (Hurrell and Deser 2010). Thus, changes in NAO seem to be inextricably linked to those observed in rainfall of some North Atlantic Ocean islands. This may be attributable to NAO impacts on trade winds (George and Saunders 2001) corresponding to higher rainfall amounts on windward slopes when such winds are stronger. Consequently, the spatial variation in extreme events of Madeira may be explained by its high dependence on the dynamic interaction of the trade winds with the island's morphology (Espinosa et al. 2020).

Although further simulations would be performed over a longer period in order to have climatological trends, the presented findings would support the management of the flash-floods natural hazard in the future due to extreme rainfall events over Madeira and Canary islands. Moreover, the findings are expected to contribute to the improvement of actions towards sustainable water management in the island and of other small islands with climatic characteristics influenced by large-scale circulation patterns.

4. Summary, challenges and links built

In this report, we have described a multi-institute effort to create a collection of high-resolution convection-permitting (CP) regional climate simulations for three outer-European domains, referred to as (1) *the Caribbean*, (2) *Madeira and Canary Islands* and (3) *la Réunion*. The simulations were not part of the original EUCP "Description of Action" and are therefore limited in scope and design. They can be considered as 'demonstrators' of the application of CP-modelling to these outer-European domains. In this last section, we look back and comment on a number of challenges met during the process of generating the simulations.

First, none of the groups had particular modelling experience at CP-scale over the new domains. In the chapter on 'la Réunion', some of the details of setting up a CP model in a new geometry are discussed. A similar endeavour was undertaken by the other contributing institutes setting up their modelling environments to new challenging domains. For the Caribbean and the island of la Réunion simulating tropical cyclones (TC) was high on the agenda. This required special care regarding the choice of the model domain geometry, such that mature TC could enter the domain from outside and have enough 'spin-up' time to adjust before hitting its main target, such as the islands. EUCP funding did not allow for a systematic re-tuning of the models and therefore an important limitation is that there is no complete overview of the models' performance via evaluation against a broad set of standard climate variables. One of the limiting factors is the availability of high quality and high-resolution observations. A recommendation for future projects would be to make sure suitable observation sets are available prior to the project (i.e., include detailed information in the proposal). This requirement will get more and more stringent as the CP-models increase their resolution.

The second challenge is how to deal with internal variability. This is a general aspect relevant to all studies that involve climate modelling, but especially important in CP modelling, where often very high resolution is preferred above a longer integration length. Especially for the Caribbean domain, which had a focus on TC as the subject of internal variability becomes tangible. TC occurrence is known for having a large internal variability, due to for example ENSO. For this reason, future changes derived from conventional time-slice-based regional climate simulation of the order of 5-10 years[9] would most likely be dominated by internal variability. In an attempt to reduce the effect of internal variability, the institutes running the Caribbean domain decided to use a *Pseudo Global Warming* (PGW) approach. In the PGW approach, a future-change signal is added to historic weather conditions at the boundaries of the regional model. In this way, daily historical weather is in some way 'futurized'. While the idea sounds very attractive, the practicality of 'futurizing' historical extremes – and a TC clearly falls in that category – turns out to be quite complicated. Because the PGW approach involves large-scale adjustment of temperature, moisture and circulation profiles, historic extremes have a high chance of becoming less extreme. For example, small – perhaps even random – changes in TC track location may produce large local effects. This was clearly shown by the evaluation of hurricane Irma (2017). With the present ensemble at least some of the random track variations can be examined, in combination with model spread. One important lesson is that it is almost impossible to compare historic and future storms on a case-by-case basis to infer the future changes. Even in a PGW approach,

[9] The scope that was possible with the available funding and the target resolution and domain size was around 5-10 hurricane seasons.

the cases may differ strongly due to randomly introduced changes, which only relatively large ensembles could potentially reveal. This was already noted by Gutmann et al (2018) but is also an important outcome of the present study. Generally, robust statistics can only be produced by combining data (pooling in time and space). A paper is in preparation describing outcomes of the endeavour for the Caribbean (De Vries et al., *in preparation*).

Another limitation of the PGW approach is that it cannot capture changes outside the regional modelling domain. If there are important future changes in the TC source regions off the west coast of Africa, these are not included in the PGW simulations. Finally, if the delta-change fields added to the reference simulations have a systematic bias, the response will also reflect this bias. For example, Seager et al. (2019) discovered that the CMIP5 ensemble-mean systematically overestimates the historic NINO3.4 trend, because the models are unable to resolve specific oceanic processes. This bias will likely also influence the future projections, and because El Niño is an important climate moderator in the Caribbean (TC occurrence and rainfall, to mention some important parameters), a systematic bias may be introduced by adding the CMIP5-based delta-change fields in the PGW simulations. Because all contributing groups added the same delta fields, such biases do not average out as would be the case in a conventional time-slice approach in which each institute uses its own specific GCM simulation for providing boundary conditions for the regional model. Therefore, it is important that the most robust finding for the Caribbean – a mean drying signal – is considered within this perspective. Because no other simulations at CP resolution are available, here we most likely have to rely on coarser resolution GCM information.

In contrast to the Caribbean-simulations, the simulations over la Réunion were created using a conventional time-slice approach. The dynamic downscaling reveals important small-scale differences in the future temperature and precipitation change. Also, the results noted that internal variability due to large-scale conditions is large. The role of internal variability has been made quantitative for example by pooling data over the domain and bootstrapping the results. Nevertheless, a recommendation is that longer time series and/or multi-model efforts are required to test the robustness of the results.

For Madeira and the Canary islands, a mixed approach was chosen (one institute ran a PGW experiment, the other, a time-slice experiment). Internal variability introduced by large-scale circulation modes such as NAO play a role in this region and future studies will be required to put the results into perspective.

Finally, we briefly discuss some of the links built during this project. The simulations have all been run on local supercomputer systems of the contributing institutes. Most of the data is still available after contacting the main authors. During the project a subset of the output has been made available and stored at the E-Science Centre. This data has been used by partners in WP4 for subsequent impact analysis. For the Caribbean-domain simulations, this involved setting up a storm-surge model. For storm surges, not only is the exact geometry of the islands quite important, a subtle difference of track-location, size of TC, or its intensity may also quickly induce substantial differences. Storm-surge models are usually evaluated against in-situ tide-gauge measurements. Due to the aforementioned differences, an exact matching against the observed time-series was difficult. Substantial differences already occurred in the present-day “re-simulation” of the storms, but were obviously amplified in the

PGW simulations. We had hoped that a case-based comparison would be possible, but this was not really possible. Robust results are likely only obtained after suitably combining and aggregating data in time and space.

Some future research and applications are planned that use the data obtained in this deliverable. At KNMI, a new set of climate scenarios is currently being developed. These have the Netherlands and Western Europe as their main targets. However, one chapter in this set of climate scenarios is going to be devoted to the future changes in the Caribbean (especially the BES-islands Bonaire, Sint Eustatius and Saba). Here, the CPM and RCM data will be used in combination with GCM information from CMIP6 and other high-resolution projects such as PRIMAVERA. In addition, incorporation of the WP4 impact-model results will be investigated.

5. References

Adler, R.; Wang, J.J.; Sapiano, M. et al. 2016. Global Precipitation Climatology Project (GPCP) Climate Data Record (CDR), Version 2.3 (Monthly). National Centers for Environmental Information. doi:10.7289/V56971M6

Ban, N., Caillaud, C., Coppola, E., Pichelli, E., Sobolowski, S., Adinolfi, M., ... & Zander, M. J. (2021). The first multi-model ensemble of regional climate simulations at kilometer-scale resolution, part I: evaluation of precipitation. *Climate Dynamics*, *57*(1), 275-302.

Brogli, R., N. Kröner, S. L. Sørland, D. Lüthi, C. Schär (2019). The role of Hadley circulation and lapse-rate changes for the future European summer climate. J. Climate, 32, 385-404, https://doi.org/10.1175/JCLI-D-18-0431.1

Bucchignani, E., Mercogliano, P., Panitz, H. J., Montesarchio, M. (2018). Climate change projections for the Middle East–North Africa domain with COSMO-CLM at different spatial resolutions. Advances in Climate Change Research, 9, 66-80.

Caillaud, C., Somot, S., Alias, A., Bernard-Bouissières, I., Fumière, Q., Laurantin, O., … Ducrocq, V. (2021). Modelling Mediterranean heavy precipitation events at climate scale: an object-oriented evaluation of the CNRM-AROME convection-permitting regional climate model. In Climate Dynamics (Vol. 56). https://doi.org/10.1007/s00382-020-05558-y

Carrillo, J., Guerra, J. C., Cuevas, E., Barrancos, J. (2016). Characterization of the Marine Boundary Layer and the Trade-Wind Inversion over the Subtropical North Atlantic, Boundary Layer Meteorology, 158, 311–330, https://doi.org/10.1007/s10546-015-0081-1

Déqué M, Somot S (2008) Analysis of heavy precipitation for France using high resolution ALADIN RCM simulations. Időjárás Q J Hung Meteorol Serv 112(3–4):179–190

Emanuel, K. The dependence of hurricane intensity on climate. *Nature* 326, 483–485 (1987). https://doi.org/10.1038/326483a0

Emanuel K A and Nolan D S 2004 Tropical cyclone activity and global climate. Proc. of 26th Conf. on Hurricanes and Tropical Meteorology (American Meteorological Society, Miami, FL), pp 240–1.

Espinosa, L. A. and Portela, M. M. (2020). Rainfall trends over a small island teleconnected to the North Atlantic oscillation-the case of Madeira Island, Portugal. Water Resources Management, 34, 4449-4467

Expósito, F. J., González, A., Pérez, J. C., Díaz, J. P., Taima, D. (2015). High-resolution future projections of temperature and precipitation in the Canary Islands. Journal of Climate, 28, 7846-7856

Falkland, A. and Custodio, E. (1991). Hydrology and water resources of small islands: a practical guide: a contribution to the International Hydrological Programme. Stud. Rep. Hydrol., 49, i-xiii

Fumière, Q., Déqué, M., Nuissier, O., Somot, S., Alias, A., Caillaud, C., … Seity, Y. (2019). Extreme rainfall in Mediterranean France during the fall: added value of the CNRM-AROME Convection-Permitting Regional Climate Model. Climate Dynamics. https://doi.org/10.1007/s00382-019-04898-8

Fragoso, M., Trigo, R. M., Pinto, J. G., Lopes, S., Lopes, A., Ulbrich, S., Magro, C. (2012). The 20 February 2010 Madeira flash-floods: synoptic analysis and extreme rainfall assessment. Natural Hazards and Earth System Sciences, 12, 715-730

Gao, J., Tang, G., & Hong, Y. (2017). Similarities and improvements of GPM dual-frequency precipitation radar (DPR) upon TRMM precipitation radar (PR) in global precipitation rate estimation, type classification and vertical profiling. *Remote Sensing*, *9*(11), 1–26. https://doi.org/10.3390/rs9111142

George, S. E., Saunders, M. A. (2001). North Atlantic oscillation impact on tropical North Atlantic winter atmospheric variability. Geophys. Res. Lett., 28, 1015–1018

Gilford, D. M. PyPI (v1.3): Tropical Cyclone Potential Intensity Calculations in Python. *Geosci. Model Dev.* **14**, 2351–2369 (2021).

Grubišić, V., Sachsperger, J., Caldeira, R. M. A. (2015). Atmospheric Wake of Madeira: First Aerial Observations and Numerical Simulations, Journal of the Atmospheric Sciences, 72, 4755–4776, https://doi.org/10.1175/JAS-D-14-0251.1

Gutmann, E. D. *et al.* Changes in hurricanes from a 13-Yr convection-permitting pseudo- global warming simulation. *J. Clim.* **31**, 3643–3657 (2018).

Herrera, R. G., Puyol, D. G., Martín, E. H., Presa, L. G., Rodríguez, P. R. (2001). Influence of the North Atlantic oscillation on the Canary Islands precipitation. J. Clim., 14, 3889–3903

Hurrell, J. W. and Deser, C. (2010). North Atlantic climate variability: the role of the North Atlantic oscillation. J. Mar. Syst., 79, 231–244

Jones, P. D. *et al.* Long-term trends in precipitation and temperature across the Caribbean. *Int. J. Climatol.* **36**, 3314–3333 (2016).

Knutson, T. *et al.* Tropical cyclones and climate change assessment. *Bull. Am. Meteorol. Soc.* **100**, 1987–2007 (2019).

Kossin, J. P. A global slowdown of tropical-cyclone translation speed. *Nature* **558**, 104–107 (2018).

Leutwyler, D., D. Lüthi, N. Ban, O. Fuhrer, C. Schär (2017). Evaluation of the Convection-Resolving Climate Modeling Approach on Continental Scales. J. Geophys. Res. Atmos., 122, 5237-5258, http://dx.doi.org/10.1002/2016JD026013

Lochbihler, K., Lenderink, G., & Siebesma, A. P. (2017). The spatial extent of rain- fall events and its relation to precipitation scaling. Geophysical Research Let- ters, 44(16), 8629–8636.

Madruga, L., Wallenstein, F., José Manuel N. Azevedo (2016). Regional ecosystem profile–Macaronesian Region. EU Outermost Regions and Overseas Countries and Territories. BEST, Service contract 07.0307.2013/666363/SER/B2, European Commission, p 233

Martinez, C., Goddard, L., Kushnir, Y. & Ting, M. Seasonal climatology and dynamical mechanisms of rainfall in the Caribbean. *Clim. Dyn.* **53**, 825–846 (2019).

van Oldenborgh, G. J. *et al.* Attribution of extreme rainfall from Hurricane Harvey, August 2017. *Environ. Res. Lett.* **12**, (2017).

Pérez, J., J. Díaz, A. González, J. Expósito, F. Rivera-López, D. Taima (2014). Evaluation of WRF parameterizations for dynamical downscaling in the Canary Islands. J. Climate, 27, 5611– 5631

Schär, C., Frei, C., Lüthi, D. & Davies, H. C. Surrogate climate-change scenarios for regional climate models. *Geophys. Res. Lett.* **23**, 669–672 (1996).

Schär, C., and Durran, D. R. (1997). Vortex formation and vortex shedding in continuously stratified flows past isolated topography. Journal of the atmospheric sciences, 54, 534-554

Seager, R. *et al.* Strengthening tropical Pacific zonal sea surface temperature gradient consistent with rising greenhouse gases. *Nat. Clim. Chang.* **9**, 517–522 (2019).

Séférian, R., Nabat, P., Michou, M., Saint-Martin, D., Voldoire, A., Colin, J., … Madec, G. (2019). Evaluation of CNRM Earth System Model, CNRM-ESM2-1: Role of Earth System Processes in Present-Day and Future Climate. Journal of Advances in Modeling Earth Systems, 11(12), 4182–4227. https://doi.org/10.1029/2019MS001791

Spiridonov V, Déqué M, Somot S (2005) ALADIN-CLIMATE: from the origins to present date. ALADIN Newslett 29:89–92

Termonia, P., Fischer, C., Bazile, E., Bouyssel, F., Brožková, R., Bénard, P., … Joly, A. (2018). The ALADIN System and its canonical model configurations AROME CY41T1 and ALARO CY40T1. Geoscientific Model Development, 11(1), 257–281. https://doi.org/10.5194/gmd-11-257-2018

Vecchi, G. A. & Soden, B. J. Increased tropical Atlantic wind shear in model projections of global warming. *Geophys. Res. Lett.* **34**, 1–5 (2007).

De Vries et al. (*in preparation):* Changes in Caribbean hurricanes derived from an ensemble of convection-permitting pseudo-global warming simulation.

Wang, B. & Murakami, H. Dynamic genesis potential index for diagnosing present-day and future global tropical cyclone genesis. *Environ. Res. Lett.* **15**, (2020).

World Meteorological Organisation. Atlas of Mortality and Economic Losses from Weather, Climate, and Water Extremes (1970-2019). Geneva, Switzerland: World Meteorological Organisation, 2021

6. Appendix

Caribbean: Appendix A - Availability of data

Data is available upon reasonable request at most of the contributing institutes. A common set of output data fields have been prepared (and temporarily stored at the E-Science Centre) for post-processing and impact studies by EUCP WP4. Filename conventions follow as much as possible the protocol from CORDEX-FPS Convection. The data include:

variable	frequency	runs
Mean sea level pressure (PSL)	6-hourly	REF, PGW (June-October)
Wind speed components (UAS, VAS)	hourly	REF, PGW (June-October)
Temperature (tas)	hourly	REF, PGW (June-October)
Precipitation (pr)	hourly	REF, PGW (June-October)
Short-wave radiation (rsds)	hourly	REF, PGW (June-October)

Caribbean: Appendix B - PGW delta fields

With the help of Andreas Prein, we obtained a set of files from NCAR from which the PGW delta fields have been derived by KNMI[10]. They need to be added to ERA5 boundaries:

- The set consists of 19 CMIP5-GCMs. Each GCM is represented by one member, mostly r1i1p1, but for CNRM-CM5 and HadGEM2-ES it is r2i1p1.
- The historical files contain the annual cycle at monthly resolution derived from the period 1976-2005. Likewise, the rcp85 files contain the annual cycle derived from the period 2071-2100.
- The parameters, arranged in separate files, are: ta, hur, hus, ua, va, zg (multi-level) and ps, psl, ts (single level). (ts is used for sst). All fields were remapped on a common 1x1 degree regular long-lat grid (done by NCAR). All multi-level fields are available on pressure levels. The number of pressure levels among the GCMS varies from 17 to 35, but there is a common set of 17 pressure levels: 1000, 925, 850, 700, 600, 500, 400, 300, 250, 200, 150, 100, 70, 50, 30, 20, 10 hPa.

A data set was prepared containing the multi-model perturbations (difference between RCP8.5 and historical) on a common grid. The next step is to merge the set of perturbations with the standard forcings (e.g., ERA5). Basically, there are two ways to do the merging.

7. Create two sets of lateral boundary forcings (e.g., ERA5 and ERA5+perturbations) and carry out two simulations driven by either of the two sets.
8. Have one set of lateral boundary forcings (e.g., ERA5) and carry out two simulations, like in 1). In the perturbed simulation, the perturbations are imported and merged in runtime with the

[10] The files can be downloaded from the EUCP wiki page: delta-fields

standard forcing (it requires a lot of interpolations in both space and time). At KNMI this is done through RACMO which serves as an intermediate model.

The advantage of 2) is that it is much more flexible in dealing with perturbations; there is only one large data set with ERA5-forcings, while one can easily change from one to another perturbation. The downside is that one needs to have a model that can handle the merging. It was decided that individual groups would carry out this step themselves.

Caribbean: Appendix C - Supplemental figures

Figure S1: The Caribbean domains: the minimum domain (yellow line), the ICTP domain corner points and the HCLIM CARIB03B domain (cover and extension zone shown).

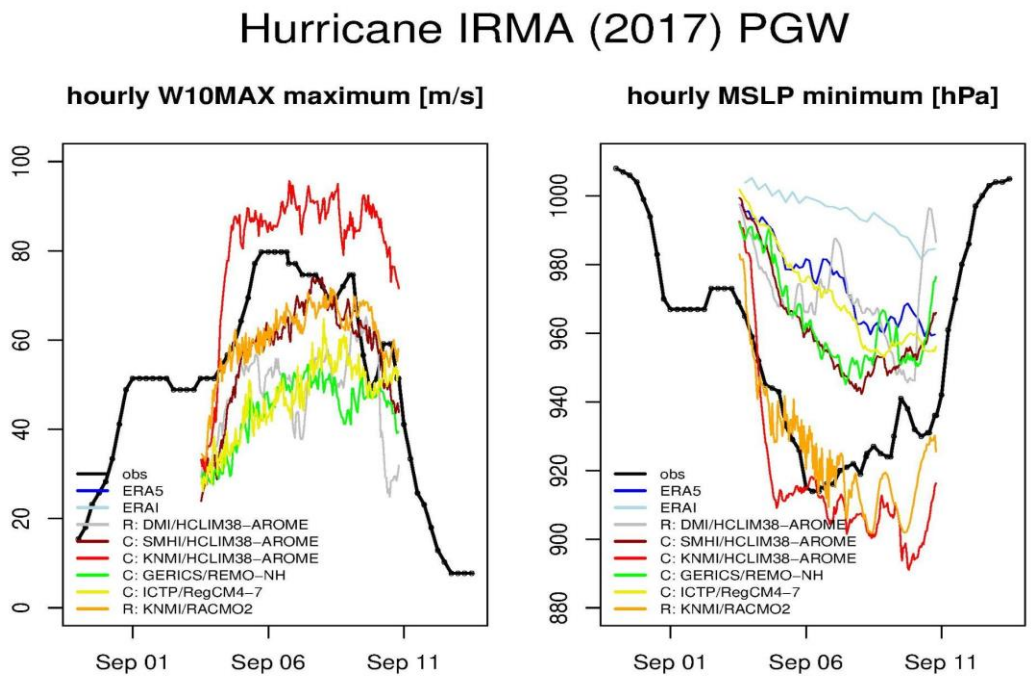

Figure S2: Evolution of Hurricane Irma under PGW. The black line (obs) and ERA5 and ERAInterim are from REF.

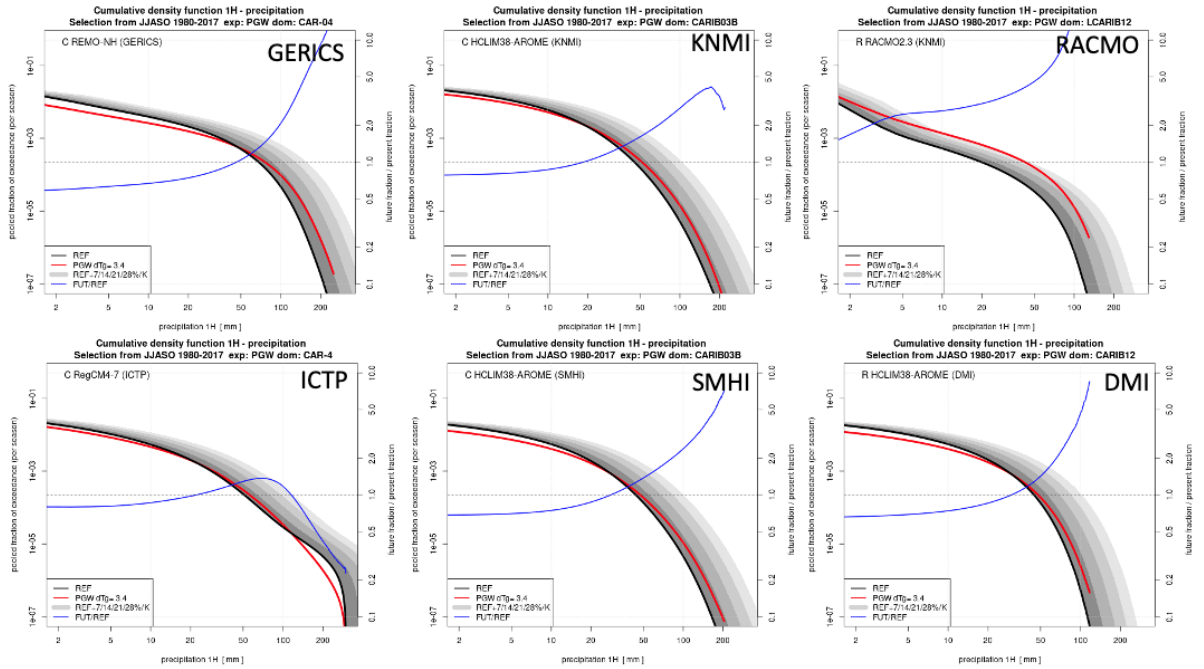

Figure S3. Hourly precipitation CDFs for all contributing models.

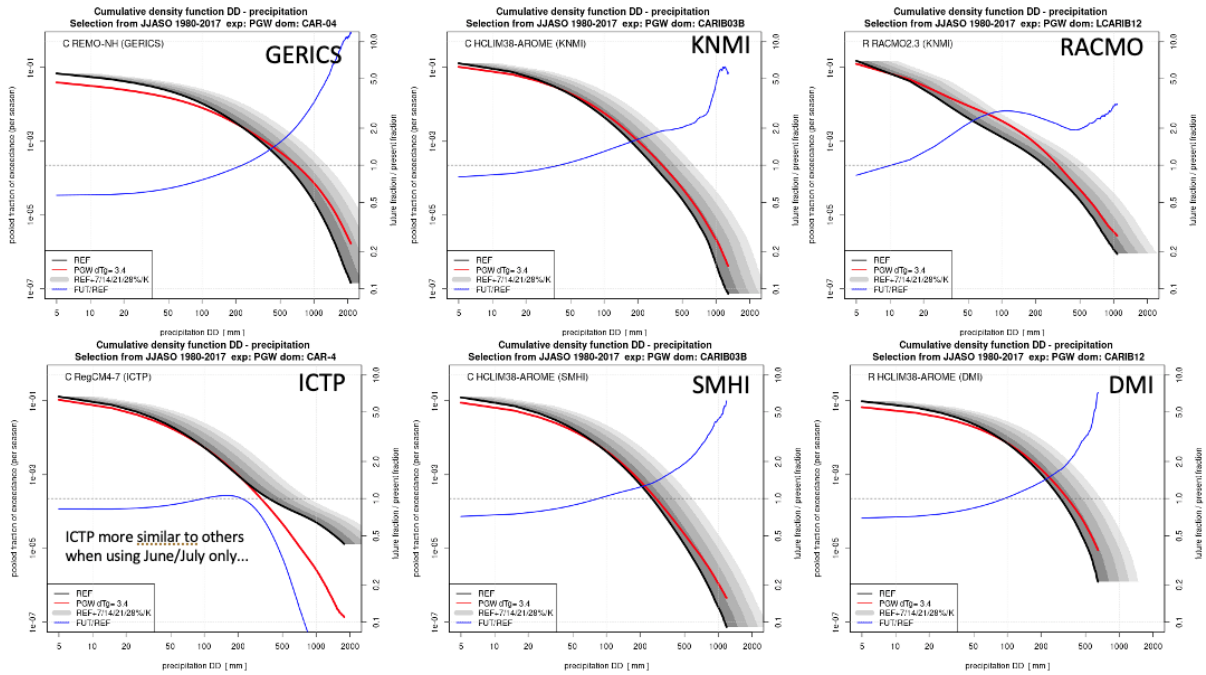

Figure S4. Daily precipitation CDFs for all contributing models.